Aus dem Institut für Schlaganfall- und Demenzforschung

Klinikum der Universität München

Effects of Amyloid and Tau Pathology on Brain Function and Cognition in Alzheimer's Disease

Dissertation

zum Erwerb des Doctor of Philosophy (Ph.D.)

an der Medizinischen Fakultät der

Ludwig-Maximilians-Universität zu München

vorgelegt von

Anna Rubinski

März 2021

Mit Genehmigung der Medizinischen Fakultät der

Ludwig-Maximilians-Universität zu München

First supervisor/reviewer: Prof. Dr. Michael Ewers

Second reviewer: Prof. Dr. med. Marco Düring

Dean: Prof. Dr. med. dent. Reinhard Hickel

Date of Defense: 07/09/2021

Table of contents

List of abbreviations

Aβ – Beta-Amyloid

AD – Alzheimer's Disease

ASL – Arterial Spin Labeling

BBB – Blood-Brain Barrier

CN – Cognitively Normal

CBF – Cerebral Blood Flow

CSF – Cerebrospinal Fluid

FDG-PET – [18F]-2-Fluoro-2-deoxy-D-glucose Positron Emission Tomography

FPCN – Frontoparietal Control Network

LFC – Left Frontal Cortex

MCI – Mild Cognitive Impairment

MRI – Magnetic Resonance Imaging

PET – Positron Emission Tomography

SVD – Small Vessel Disease

WMH – White Matter Hyperintensities

List of publications included in this thesis

Manuscript 1: Rubinski, A., Franzmeier, N., Neitzel, J., & Ewers, M. (2020). FDG-PET hypermetabolism is associated with higher tau-PET in mild cognitive impairment at low amyloid-PET levels. *Alzheimer's research & therapy, 12*(1), 1-12.
DOI: 10.1186/s13195-020-00702-6.

Manuscript 2: Rubinski, A., Tosun, D., Franzmeier, N., Neitzel, J., Frontzkowski, L., Weiner, M., & Ewers, M. (2021). Lower cerebral perfusion is associated with tau-PET in the entorhinal cortex across the Alzheimer's continuum. *Neurobiology of Aging, 102*, 111-118.
DOI: 10.1016/j.neurobiolaging.2021.02.003

Manuscript 3: Neitzel, J., Franzmeier, N., **Rubinski, A.,** Ewers, M., & Alzheimer's Disease Neuroimaging Initiative (ADNI). (2019). Left frontal connectivity attenuates the adverse effect of entorhinal tau pathology on memory. *Neurology, 93*(4), e347-e357.
DOI: 10.1212/WNL.0000000000007822

Overview

The pathophysiological process in Alzheimer's disease (AD), namely the accumulation of beta-amyloid (Aβ) plaques and tau neurofibrillary tangles, begins decades before the initial clinical symptoms occur. The accumulation of both pathologies is considered to play a significant role in the neurodegenerative cascade leading to loss of neurons and synapses and ultimately affecting brain function and cognition in AD. Based on the disease stage and AD pathology levels, Aβ-plaques and pathologic tau may have a unique or synergistic effect on brain function and cognition.

In this thesis, using advanced multimodal neuroimaging techniques, we explore the complex pathophysiology of AD by studying the association between PET tracers of Aβ and pathologic tau, brain function, and cognition across the AD spectrum. As measures of brain function, we focused on glucose metabolism assessed by FDG-PET (manuscript 1) and cerebral perfusion assessed by ASL-MRI (manuscript 2). Although glucose metabolism and cerebral perfusion both reflect neuronal function and therefore are tightly coupled in the brain, each measure provides unique characteristic spatiotemporal information based on the stage of the disease and the biomarker levels. Since the extent of cognitive impairment may vary substantially between different individuals, we took the next step to identify functional brain alterations that may explain those variations. We focused on the global connectivity of the left frontal cortex, a proxy measure underlying cognitive reserve, and tested whether it attenuates the adverse effect of AD pathologies on cognitive performance (manuscript 3).

Introductory summary

1. Sporadic Alzheimer's disease

Alzheimer's disease (AD) is a progressive neurodegenerative disease. It accounts for 60-70% of all dementia cases, with an increasing incidence rate with the age of the individuals, especially over the age of 65 (Kukull *et al.*, 2002). AD usually manifests clinically with incidental forgetfulness at the initial stage. This stage can last 2-3 decades, during which individuals are still cognitively normal (CN) but start to accumulate beta-amyloid (Aβ) plaques and tau neurofibrillary tangles (Jack *et al.*, 2010). Next, the disease progresses to mild cognitive impairment (MCI) stage which is characterized by episodic memory dysfunction and the inability to form new memories. This stage can last up to several years during which AD primary pathologies continue to accumulate. Finally, the majority of individuals with MCI will advance to full-blown AD dementia, which is defined as impairments in multiple domains including a severe decline in cognitive functions, personality, and behavioral changes (Albert *et al.*, 2011; Dubois *et al.*, 2016; Jack *et al.*, 2018).

While clinical symptoms are indicative of AD onset, the diagnosis of AD can be performed using an unbiased descriptive classification scheme, labeled - AT(N). The AT(N) system utilizes both fluid and imaging biomarkers and is referring to three pathologic processes which are evident in AD, including extracellular Aβ-plaques (A), intracellular neurofibrillary tau tangles (T) and, neurodegeneration (N) (Jack *et al.*, 2018). While positive Aβ biomarkers are necessary to place an individual in the AD-continuum, tau biomarkers determine whether the individual has AD, since both biomarkers are required for neuropathological diagnosis of the disease. Finally, neurodegeneration biomarkers and cognitive symptoms provide non-specific information and are used only to stage disease severity.

2. Biomarkers of Aβ and tau pathology

Aβ-plaques and tau neurofibrillary tangles are the pathologic hallmarks of AD. Aβ is created from the abnormal cleavage of Aβ precursor protein by beta- and gamma-secretases (Esch *et al.*, 1990; Selkoe, 1998). There are two major Aβ isoforms: Aβ40 and Aβ42, with Aβ42 isoform being the main constituent of Aβ-plaques in AD brains (Miller *et al.*, 1993; Gravina *et al.*, 1995)

due to its low solubility and propensity to form aggregates with β-pleated sheet structure (Gu and Guo, 2013). Tau is a soluble microtubule-associated protein which under normal physiological conditions stabilizes intracellular microtubules (Binder *et al.*, 1985; Black *et al.*, 1996). In a disease state, tau is abnormally hyperphosphorylated, which leads to its detachment from the microtubule, loss of normal function, and promotes its self-aggregation (Lee *et al.*, 2001). Abnormal tau is toxic to neurons and may further aggregate into paired helical filaments and neurofibrillary tangles, the key neuropathological feature in AD (Trojanowski and Lee, 1995; Ballatore *et al.*, 2007).

Both Aβ and tau pathologies can be measured using either fluid or neuroimaging biomarkers. However, anatomical information from imaging provides an advantage for imaging over fluid biomarkers since it can help to distinguish both temporally and anatomically between different disease stages. The visualization and quantification of Aβ and tau biomarkers can be performed by positron emission tomography (PET) imaging (Klunk *et al.*, 2004; Wong *et al.*, 2010; Chien *et al.*, 2013; Okamura *et al.*, 2014). PET uses radiolabeled Aβ or tau precursors that cross the blood-brain barrier (BBB) and bind neuritic and diffuse Aβ-plaques or tau neurofibrillary tangles, respectively.

The relationship between Aβ and pathologic tau on the one hand, and functional brain changes and cognition on the other hand, are incompletely understood. Although elevated Aβ levels may be indicative of future cognitive decline, the effect of Aβ on cognition appears to be mainly driven by neurodegenerative changes (Huijbers *et al.*, 2014; Villeneuve *et al.*, 2014). Moreover, results from histochemical post-mortem and PET studies suggest that in contrast to Aβ, the spatial patterns of tau tracer uptake are highly correlated with the patterns of neurodegeneration and clinical progression (Bischof *et al.*, 2016; Ossenkoppele *et al.*, 2016; Schöll *et al.*, 2016; Dronse *et al.*, 2017; Iaccarino *et al.*, 2018; La Joie *et al.*, 2020). Specifically, tau-PET uptake patterns closely match regional cross-sectional (Gordon *et al.*, 2018) as well as longitudinal grey matter atrophy (La Joie *et al.*, 2020) and reduced glucose metabolism (Bischof *et al.*, 2016; Ossenkoppele *et al.*, 2016). As for cognition, pathologic tau assessed by tau-PET specifically in the entorhinal cortex is associated with early episodic memory impairment (Schöll *et al.*, 2016; Xia *et al.*, 2017; Maass *et al.*, 2018) and both baseline and changes in tau-PET are related to changes in cognition (Pontecorvo *et al.*, 2019). Therefore, tau is the major driver of structural alterations and cognitive decline in AD.

3. Functional brain alterations in Alzheimer's disease

As structural alterations and cognitive decline are rather late events in the neurodegenerative cascade, changes detectable with functional imaging may provide a useful biomarker to assess the early effects of primary AD pathologies. Numerous functional imaging methods have been developed to investigate early pathological changes and are primarily based on the connection between neural activity, glucose metabolism, and blood flow.

3.1. FDG-PET metabolism

Mapping glucose metabolism, the main energy substrate of the brain, is possible using the artificial glucose analog [^{18}F]-2-Fluoro-2-deoxy-D-glucose (FDG; Phelps *et al.*, 1979), in which, the [^{18}F] substitute the normal hydroxyl at the second carbon position. After injection into the blood, similar to glucose, FDG is actively transported across the BBB and phosphorylated in the tissue. However, because of the missing oxygen, phosphorylated FDG cannot metabolize further and becomes essentially "trapped" in the tissue (Mosconi, 2013; Young *et al.*, 2020). Therefore, FDG uptake by the tissue is indicative of glucose metabolic rate. Since regional glucose metabolism is closely related to neuronal and synaptic activity (Rocher *et al.*, 2003), FDG-PET may detect synaptic dysfunction by identifying regions with reduced glucose metabolism (Mosconi, 2005).

Reductions in glucose metabolism (i.e., Hypometabolism) are useful in detecting preclinical stages of AD and are highly correlated with disease severity (Mosconi, 2005). Hypometabolism in AD is detected by a lower FDG-PET uptake predominantly in the temporo-parietal, frontal, and posterior cingulate cortices (Minoshima *et al.*, 1997; Mosconi, 2005). These patterns of hypometabolism are commonly observed not only in patients with AD dementia but also in CN elderly individuals which are Aβ-positive (Lowe *et al.*, 2014), individuals at genetic risk of AD (Small *et al.*, 1995), as well as in individuals with MCI (Anchisi *et al.*, 2005). Moreover, the characteristic patterns of AD neurodegeneration appear earlier on FDG-PET than on MRI and are predictive of the progression from MCI to AD dementia (Shaffer *et al.*, 2013; Blazhenets *et al.*, 2019).

Although FDG-PET hypometabolism was predominantly observed in Aβ-positive individuals and therefore was attributed to elevations in global amyloid-PET levels (Edison *et al.*, 2007;

Ewers *et al.*, 2012; Lowe *et al.*, 2014), there is a weak spatial correspondence between the patterns of amyloid-PET deposition and FDG-PET metabolism (Li *et al.*, 2008; Rabinovici *et al.*, 2008). Suggesting that amyloid-PET alone may not be directly responsible for FDG-PET deficits in AD. In fact, multiple neuroimaging studies recently showed that in prodromal and AD dementia, tau-PET is strongly associated with regionally matching decreases in FDG-PET metabolism (Bischof *et al.*, 2016; Ossenkoppele *et al.*, 2016; Dronse *et al.*, 2017; Whitwell *et al.*, 2018).

Interestingly, during the course of AD, FDG-PET metabolism shows complex non-linear changes, including stages of reduced as well as increased (i.e., hypermetabolism) FDG-PET metabolism. While several studies have found an association between Aβ-deposition and hypermetabolism in CN individuals (Johnson *et al.*, 2014; Oh *et al.*, 2014) and individuals with MCI (Cohen *et al.*, 2009), others have shown that hypermetabolism is independent of Aβ pathology in CN individuals at genetic risk of AD (Benzinger *et al.*, 2013; Yi *et al.*, 2014), and MCI (Ashraf *et al.*, 2015). The apparently contradicting findings could result from an association between amyloid and tau pathology. In CN individuals, the relationship between tau-PET and FDG-PET metabolism appears to be dependent on amyloid-PET levels. Specifically, at low amyloid-PET, a positive association between tau-PET and FDG-PET metabolism is observed, while at high amyloid-PET this association becomes negative or no longer significant (Hanseeuw *et al.*, 2017; Adams *et al.*, 2018). Similarly, at more severe disease stages, high amyloid-PET levels are associated with a negative relationship between tau-PET and FDG-PET metabolism (Bischof *et al.*, 2016).

Taken together, stages of hyper- and hypometabolism are observed across the spectrum of AD and may be driven by the dynamic association between amyloid and tau pathology. How exactly these pathologies affect metabolism and whether there is indeed an abnormal increase in metabolism in MCI is currently unknown. Moreover, while it is clear that reductions in metabolism have detrimental effects and are predictive of disease severity (Mosconi, 2005), and cognitive decline in early (Mosconi *et al.*, 2008) as well as in late disease stages (Landau *et al.*, 2012), the effects of increases in metabolism are unclear.

Therefore, in manuscript 1 we assessed the contribution of amyloid- and tau-PET to FDG-PET alterations in symptomatic elderly subjects (i.e., MCI), by assessing the main effect as well as the interaction between the pathologies. Next, as increases in metabolism can be interpreted

either as a compensatory response in order to maintain cognition or as an early excitotoxic disease process, we sought to determine whether increased FDG-PET metabolism is in fact abnormally high compared to healthy controls and whether it is beneficial or detrimental for cognitive performance.

In the first study (manuscript 1), we observed that alterations in FDG-PET metabolism (i.e., stages of hypo- and hypermetabolism) in symptomatic elderly subjects are dependent on regional amyloid- and tau-PET levels. Specifically, we found that while FDG-PET is highly correlated with tau-PET levels, the direction of the association is dependent on regional amyloid-PET levels. When amyloid-PET levels are low, tau-PET is positively associated with FDG-PET, whereas at higher amyloid-PET levels, the association between tau-PET and FDG-PET becomes non-significant or negative. Furthermore, we show that the positive association between tau-PET and FDG-PET metabolism is indicative of abnormally elevated metabolism levels compared to healthy controls and in turn is associated with worse cognitive performance.

3.2. Cerebral perfusion

Another functional brain alteration observed in AD is reduced cerebral perfusion (Prohovnik *et al.*, 1988). Cerebral perfusion designates the blood supply of the microvasculature in the brain, which is important for oxygen and glucose supply as well as clearance of waste substances (Iadecola, 2013; Fantini *et al.*, 2016). Disruption of the blood supply to the brain cells may cause a deficiency in oxygen and glucose, inevitably leading to neuronal dysfunction (Iadecola, 2013; Fantini *et al.*, 2016). Since neuronal dysfunction is an early event in AD, which eventually may lead to cognitive impairment and neurodegeneration, there is a clear need to be able to detect early disruptions in perfusion. The most common way to measure cerebral perfusion is as cerebral blood flow (CBF) which refers to the rate of delivered arterial blood to brain tissue (Liu and Brown, 2007). While CBF is typically measured using [^{15}O]-water-PET imaging or single-photon emission computed tomography (SPECT), it can also be non-invasively measured using arterial spin labeling (ASL) MRI.

ASL is a radiation-free MRI technique that measures CBF by magnetically labeling the protons of arterial blood water flowing into the brain tissue, thus eliminating the need for an external

tracer or a contrast agent. ASL shows reliable measurements of CBF in young and elderly adults with high spatial correlation with CBF measured by exogenous contrast agents, such as [^{15}O]-water-PET (Xu *et al.*, 2010; Kilroy *et al.*, 2014). ASL is easy to implement in routine MRI scans and shows reproducibility in multicenter studies (Petersen *et al.*, 2010; Gevers *et al.*, 2011). Therefore, ASL-MRI serves as a clinically attractive marker over radioactive methods for visualization and quantification of CBF.

In AD, CBF is typically disrupted and most commonly reduced (i.e., hypoperfusion) in the temporo-parietal and the posterior cingulate cortex (Johnson *et al.*, 2005; Dai *et al.*, 2009; Binnewijzend *et al.*, 2013; Binnewijzend *et al.*, 2016). CBF differs as a function of AD risk and can differentiate between CN individuals, adults at risk, or patients diagnosed with AD (Wierenga *et al.*, 2012; Wierenga *et al.*, 2013; Okonkwo *et al.*, 2014). Furthermore, lower CBF is associated with worse cognitive performance throughout the AD continuum (Chao *et al.*, 2010; Leijenaar *et al.*, 2017). Taken together, evidence suggests that CBF plays a role in maintaining cognitive function and disease progression, and therefore can be useful as a preclinical biomarker of AD.

A substantial body of work describes the relationship between Aβ accumulation and CBF, including recent neuroimaging studies in which, increasing levels of Aβ were associated with reduced CBF in sporadic AD (Mattsson *et al.*, 2014; Tosun *et al.*, 2014; Michels *et al.*, 2016) as well as in familial AD (McDade *et al.*, 2014; Yan *et al.*, 2017). Yet, accumulating evidence from CSF biomarkers studies show that tau proteins and not Aβ are related to CBF reductions in CN individuals (Stomrud *et al.*, 2012), individuals at genetic risk for AD (Hays *et al.*, 2020), and individuals with MCI or AD dementia (Habert *et al.*, 2010). It also appears that the pattern of CBF reductions in AD is related to the spatial distribution of tau neurofibrillary tangles, i.e., Braak stages (Bradley *et al.*, 2002). This was further corroborated in a recent mouse tauopathy model, in which, tau contributed to neurovascular alterations by interfering with the normal CBF dynamics in the brain (Park *et al.*, 2020). These observations suggest that in AD tau pathology may play an important role in CBF alterations, however, no study has yet explored the spatial relationship between tau-PET and CBF.

It is also important to note that small vessel disease (SVD) may play a role in CBF alterations, as it may reduce or interrupt perfusion to the affected regions. However, evidence regarding the associations between SVD and CBF is inconsistent. While some studies have observed

reduced CBF as a result of higher number of microbleeds (Gregg *et al.*, 2015) or higher white matter hyperintensities (WMH) volume (Crane *et al.*, 2015; Shi *et al.*, 2016; Kim *et al.*, 2020), others have found no association between CBF and overall SVD burden (Onkenhout *et al.*, 2020). Yet, considering that SVD may promote tau accumulation (Kim *et al.*, 2018; Laing *et al.*, 2020), it is important to assess the effect of SVD on the relationship between tau-PET and CBF.

Therefore, in manuscript 2, we explored the regional associations between CBF and biomarkers of amyloid and tau pathology, across the AD continuum. Given the different spatial accumulation of each pathology, we tested the independent effect of each pathology in its predilection regions as well as the interaction between the pathologies. Finally, we tested the effect of SVD on CBF alterations using MRI markers of SVD such as cerebral microbleeds and WMH.

In the second study (manuscript 2) we found that alterations in CBF can be observed in a biomarker dependent manner preferentially in each pathology predilection regions. We expand over previously reported by showing that in addition to amyloid-PET, in the entorhinal cortex, tau-PET is associated with reduced CBF. This association was independent of Aβ pathology, and no interaction between the pathologies was observed. Finally, tau related CBF reductions were evident across the AD continuum, in early as well as in late disease stages, and were independent of SVD markers.

4. Modulating the effect of primary AD pathologies

Changes in brain function as a result of Aβ plaques and tau neurofibrillary tangles accumulation may lead to cognitive impairment and eventually dementia. However, the susceptibility to AD-related pathology may vary between individuals, as it seems that some individuals are able to tolerate more pathology while still maintaining normal function (Stern, 2012). Furthermore, different individuals at a given level of primary AD pathologies may present substantial variance in the extent of cognitive impairment (Vemuri *et al.*, 2011). These individual differences are due to higher resilience or higher reserve capacity against the effect of AD-related pathology (Park and Reuter-Lorenz, 2009; Stern, 2012). Therefore, higher reserve capacity may modulate the negative effect of AD-related pathology and alleviate the cognitive impairment (Stern, 2002, 2012; Cabeza *et al.*, 2018).

While environmental factors such as education, occupation, and leisure activity can provide a reserve against AD-related pathology (Stern, 2002; Stern, 2009; Stern, 2012), the underlying mechanisms are largely unknown. Currently, it is believed that cognitive reserve acts by recruiting alternate neural networks or utilizing existing networks more efficiently to help maintain cognitive function despite brain pathology (Stern, 2009). Indeed, brain activation patterns that reflect higher neural efficiency have been observed in individuals with higher cognitive reserve (Bartrés-Faz and Arenaza-Urquijo, 2011; Barulli and Stern, 2013).

A potential neural substrate of reserve is functional connectivity within major hubs of cognitive control networks (Serra *et al.*, 2017). More specifically, higher global connectivity of the left frontal cortex (gLFC), a major hub of the frontoparietal control network (FPCN) (Cole *et al.*, 2012; Cole *et al.*, 2013), has been previously suggested to underlie cognitive reserve (Franzmeier *et al.*, 2017; Franzmeier *et al.*, 2018a; Franzmeier *et al.*, 2018b). Higher gLFC, assessed by resting-state fMRI, was associated with higher education and attenuated effect of FDG-PET hypometabolism on memory performance (Franzmeier *et al.*, 2017).

Although Aβ deposition plays an important role in the pathophysiology of AD, the associations between Aβ plaques and cognitive impairment are rather weak (Nelson *et al.*, 2012; Hedden *et al.*, 2013; Huber *et al.*, 2018). Instead, neuropathological data showed that neurofibrillary tangles are a stronger predictor of cognitive decline and therefore mediate the effect of amyloid on cognition (Giannakopoulos *et al.*, 2003; Bennett *et al.*, 2004). This was later confirmed in neuroimaging studies in which entorhinal tau-PET appeared to be a strong predictor of episodic-memory performance in CN individuals (Schöll *et al.*, 2016; Maass *et al.*, 2018) as well as in individuals with MCI and AD dementia (Bejanin *et al.*, 2017).

Recent PET studies have found that individuals with higher reserve capacity show tolerance against tau pathology (Hoenig *et al.*, 2017; Rentz *et al.*, 2017). However, in those studies, reserve was assessed through non-specific proxies such as IQ or education, which lack mechanistic insight. On the other hand, functional connectivity extends the concept of reserve to functional brain mechanisms within neural networks (Bartrés-Faz and Arenaza-Urquijo, 2011; Barulli and Stern, 2013). Whether individuals with increased functional connectivity within networks associated with reserve show higher tolerance against tau pathology is currently unknown.

Therefore, in manuscript 3, we tested whether higher functional connectivity within networks associated with cognitive reserve may attenuate the adverse effect of pathologic tau in non-demented individuals. To that end, we tested the interaction between gLFC connectivity and tau-PET in the entorhinal cortex on cognitive performance.

In the third study (manuscript 3) we found a significant gLFC connectivity by entorhinal tau-PET interaction on memory in non-demented individuals. In which, individuals with higher gLFC connectivity showed attenuated effect of entorhinal tau on memory performance compared to individuals with lower gLFC connectivity. The interaction was specific to tau pathology, as it was not significant for amyloid-PET, and it extends to the whole FPCN which the LFC is a part of. Together, these findings suggest that higher reserve capacity as expressed by higher connectivity of the FPCN and in particular of its LFC hub attenuates the negative effect of entorhinal tau-PET on cognitive performance.

Discussion and Conclusions

The major findings of the current thesis were 1) abnormally increased FDG-PET is related to higher tau-PET at low but not high amyloid-PET levels, which in turn is associated with worse cognitive performance 2) tau-PET is a major driver of CBF reductions in early Braak stages 3) the adverse effect of pathologic tau in the entorhinal cortex on cognitive performance is attenuated by higher gLFC connectivity.

While non-linear changes in FDG-PET metabolism have been previously observed in CN individuals (Hanseeuw *et al.*, 2017; Adams *et al.*, 2018), our first study extends the findings to individuals with MCI and sheds light on the pathophysiological mechanisms underlying these changes. We found that local increases in FDG-PET metabolism are driven by high levels of spatially matching tau-PET and low levels of regional amyloid-PET. The relationship between tau and increased FDG-PET metabolism could be due to tau-induced disruption of inhibitory neurotransmission which may cause hyperexcitability of cortical circuits (Levenga *et al.*, 2013; Shimojo *et al.*, 2020). We further demonstrated that FDG-PET hypermetabolism is related to worse memory performance, indicating that abnormally increased FDG-PET metabolism levels are detrimental for cognition. Together, our results suggest that tau-related FDG-PET hypermetabolism may be an early event leading to progressive neurodegeneration and cognitive decline.

Our second study revealed that tau pathology drives CBF reductions in early Braak stages. The association between pathologic tau and CBF is independent of Aβ pathology and diagnosis as it is detectable in early as well as in late disease stages. The exact mechanisms behind the effect of pathologic tau on CBF alterations are yet to be established. Tau pathology likely takes part in early vascular alterations that lead to hypoperfusion and ultimately neurodegeneration. This is supported by a recent in-vivo study in which aged tau-overexpressing mice developed blood vessel abnormalities and disrupted blood flow that in turn lead to neurodegeneration (Bennett *et al.*, 2018). Together, our results suggest that across the AD continuum, functional brain alterations as observed by reduced CBF, are tau-dependent in areas of high tau accumulation.

Pathologic tau is a major driver of cognitive decline (Schöll *et al.*, 2016; Bejanin *et al.*, 2017; Maass *et al.*, 2018). However, the adverse effects of tau pathology on cognition can be attenuated by protective functional brain mechanisms which render individuals less susceptible to pathological brain changes. In the current thesis, we took the crucial next step to identify those functional brain mechanisms that may explain tolerance to tau pathology. Our third study revealed that individuals with higher connectivity of the FPCN and in particular of its LFC hub, show attenuated effect of entorhinal tau-PET on memory performance. Thus, providing an insight into a functional brain mechanism that enhances tolerance against the negative effect of pathologic tau in the entorhinal cortex.

In conclusion, in this thesis we show that while pathologic tau is a major driver of early functional alterations in the AD neurodegenerative cascade, its effect may be dependent on the dynamic associations with Aβ-plaques. However, the detrimental effect of pathologic tau on cognition may be attenuated by protective functional brain mechanisms.

Outlook

The findings of this thesis contribute to the understanding of the complex pathophysiology of Alzheimer's disease and therefore have implications for clinical trials in terms of design and methodology. First, our results suggest that both Aβ plaques and tau neurofibrillary tangles should be targeted for effective treatment of AD since they act both independently and synergistically as a function of disease stage and biomarker levels. Second, when FDG-PET is used as an outcome measure, it is important to consider that depending on the levels of Aβ and tau biomarkers, FDG-PET metabolism may not only be reduced but also increased. This is of main importance since a beneficial drug or treatment may not necessarily reduce the decline of FDG-PET, but could also reduce the harmful increase in FDG-PET (Rubinski *et al.*, 2020). Similarly, when cognition is used as an outcome measure, reserve capacity should be recognized as a factor that might influence rates of cognitive decline. This is of main importance in studies that rely on differences in the rate of cognitive decline between patients on drug and placebo. Finally, ASL-MRI is a sensitive technique to identify not only Aβ-induced CBF alterations but also CBF reductions due to early tau deposition. For patients that are undergoing an MRI scan, ASL technique is a promising replacement for PET imaging as it may provide similar diagnostic utility and does not require exposure of the patient to radiation. Therefore, ASL-assessed CBF can serve as a non-invasive biomarker for identifying candidates in preclinical phases of the disease, as well as for testing the beneficial effects of anti-tau/anti-amyloid therapies.

The current findings may be a starting point for longitudinal studies on biomarker trajectories to further elucidate the mechanisms by which Aβ and tau pathology affect brain function and cognition over time. Future studies should also assess the influence of various modifiers, such as cognitive reserve, vascular pathology, and genetics on biomarker trajectories and outcomes. Thus, paving the way to personalized medicine based on the individual characteristics of each patient.

References

Adams JN, Lockhart SN, Li L, Jagust WJ. Relationships Between Tau and Glucose Metabolism Reflect Alzheimer's Disease Pathology in Cognitively Normal Older Adults. Cerebral Cortex 2018: bhy078-bhy.

Albert MS, DeKosky ST, Dickson D, Dubois B, Feldman HH, Fox NC*, et al.* The diagnosis of mild cognitive impairment due to Alzheimer's disease: recommendations from the National Institute on Aging-Alzheimer's Association workgroups on diagnostic guidelines for Alzheimer's disease. Alzheimer's & dementia : the journal of the Alzheimer's Association 2011; 7(3): 270-9.

Anchisi D, Borroni B, Franceschi M, Kerrouche N, Kalbe E, Beuthien-Beumann B*, et al.* Heterogeneity of Brain Glucose Metabolism in Mild Cognitive Impairment and Clinical Progression to Alzheimer Disease. JAMA Neurology 2005; 62(11): 1728-33.

Ashraf A, Fan Z, Brooks DJ, Edison P. Cortical hypermetabolism in MCI subjects: a compensatory mechanism? European Journal of Nuclear Medicine and Molecular Imaging 2015; 42(3): 447-58.

Ballatore C, Lee VMY, Trojanowski JQ. Tau-mediated neurodegeneration in Alzheimer's disease and related disorders. Nature Reviews Neuroscience 2007; 8(9): 663-72.

Bartrés-Faz D, Arenaza-Urquijo EM. Structural and Functional Imaging Correlates of Cognitive and Brain Reserve Hypotheses in Healthy and Pathological Aging. Brain Topography 2011; 24(3): 340.

Barulli D, Stern Y. Efficiency, capacity, compensation, maintenance, plasticity: emerging concepts in cognitive reserve. Trends Cogn Sci 2013; 17(10): 502-9.

Bejanin A, Schonhaut DR, La Joie R, Kramer JH, Baker SL, Sosa N*, et al.* Tau pathology and neurodegeneration contribute to cognitive impairment in Alzheimer's disease. Brain 2017; 140(12): 3286-300.

Bennett DA, Schneider JA, Wilson RS, Bienias JL, Arnold SE. Neurofibrillary Tangles Mediate the Association of Amyloid Load With Clinical Alzheimer Disease and Level of Cognitive Function. Archives of Neurology 2004; 61(3): 378-84.

Bennett RE, Robbins AB, Hu M, Cao X, Betensky RA, Clark T*, et al.* Tau induces blood vessel abnormalities and angiogenesis-related gene expression in P301L transgenic mice and human Alzheimer's disease. Proceedings of the National Academy of Sciences of the United States of America 2018; 115(6): E1289-E98.

Benzinger TLS, Blazey T, Jack CR, Koeppe RA, Su Y, Xiong C*, et al.* Regional variability of imaging biomarkers in autosomal dominant Alzheimer's disease. Proceedings of the National Academy of Sciences of the United States of America 2013; 110(47): E4502-E9.

Binder LI, Frankfurter A, Rebhun LI. The distribution of tau in the mammalian central nervous system. J Cell Biol 1985; 101(4): 1371-8.

Binnewijzend MA, Kuijer JP, Benedictus MR, van der Flier WM, Wink AM, Wattjes MP*, et al.* Cerebral blood flow measured with 3D pseudocontinuous arterial spin-labeling MR imaging in Alzheimer disease and mild cognitive impairment: a marker for disease severity. Radiology 2013; 267(1): 221-30.

Binnewijzend MAA, Benedictus MR, Kuijer JPA, van der Flier WM, Teunissen CE, Prins ND*, et al.* Cerebral perfusion in the predementia stages of Alzheimer's disease. European radiology 2016; 26(2): 506-14.

Bischof GN, Jessen F, Fliessbach K, Dronse J, Hammes J, Neumaier B*, et al.* Impact of tau and amyloid burden on glucose metabolism in Alzheimer's disease. Annals of Clinical and Translational Neurology 2016; 3(12): 934-9.

Black MM, Slaughter T, Moshiach S, Obrocka M, Fischer I. Tau is enriched on dynamic microtubules in the distal region of growing axons. J Neurosci 1996; 16(11): 3601-19.

Blazhenets G, Ma Y, Sörensen A, Rücker G, Schiller F, Eidelberg D*, et al.* Principal Components Analysis of Brain Metabolism Predicts Development of Alzheimer Dementia. Journal of nuclear medicine : official publication, Society of Nuclear Medicine 2019; 60(6): 837-43.

Bradley KM, O'Sullivan VT, Soper NDW, Nagy Z, King EMF, Smith AD*, et al.* Cerebral perfusion SPET correlated with Braak pathological stage in Alzheimer's disease. Brain 2002; 125(8): 1772-81.

Cabeza R, Albert M, Belleville S, Craik FIM, Duarte A, Grady CL*, et al.* Maintenance, reserve and compensation: the cognitive neuroscience of healthy ageing. Nat Rev Neurosci 2018; 19(11): 701-10.

Chao LL, Buckley ST, Kornak J, Schuff N, Madison C, Yaffe K*, et al.* ASL perfusion MRI predicts cognitive decline and conversion from MCI to dementia. Alzheimer Dis Assoc Disord 2010; 24(1): 19-27.

Chien DT, Bahri S, Szardenings AK, Walsh JC, Mu F, Su MY*, et al.* Early clinical PET imaging results with the novel PHF-tau radioligand [F-18]-T807. Journal of Alzheimer's disease : JAD 2013; 34(2): 457-68.

Cohen AD, Price JC, Weissfeld LA, James J, Rosario BL, Bi W*, et al.* Basal Cerebral Metabolism May Modulate the Cognitive Effects of Aβ in Mild Cognitive Impairment: An Example of Brain Reserve. The Journal of neuroscience : the official journal of the Society for Neuroscience 2009; 29(47): 14770.

Cole MW, Reynolds JR, Power JD, Repovs G, Anticevic A, Braver TS. Multi-task connectivity reveals flexible hubs for adaptive task control. Nature neuroscience 2013; 16(9): 1348-55.

Cole MW, Yarkoni T, Repovs G, Anticevic A, Braver TS. Global connectivity of prefrontal cortex predicts cognitive control and intelligence. The Journal of neuroscience : the official journal of the Society for Neuroscience 2012; 32(26): 8988-99.

Crane D, Black S, Ganda A, Mikulis D, Nestor S, Donahue M*, et al.* Gray matter blood flow and volume are reduced in association with white matter hyperintensity lesion burden: a cross-sectional MRI study. Frontiers in Aging Neuroscience 2015; 7: 131.

Dai W, Lopez OL, Carmichael OT, Becker JT, Kuller LH, Gach HM. Mild cognitive impairment and alzheimer disease: patterns of altered cerebral blood flow at MR imaging. Radiology 2009; 250(3): 856-66.

Dronse J, Fliessbach K, Bischof GN, von Reutern B, Faber J, Hammes J*, et al.* In vivo Patterns of Tau Pathology, Amyloid-beta Burden, and Neuronal Dysfunction in Clinical Variants of Alzheimer's Disease. J Alzheimers Dis 2017; 55(2): 465-71.

Dubois B, Hampel H, Feldman HH, Scheltens P, Aisen P, Andrieu S*, et al.* Preclinical Alzheimer's disease: Definition, natural history, and diagnostic criteria. Alzheimer's & dementia : the journal of the Alzheimer's Association 2016; 12(3): 292-323.

Edison P, Archer HA, Hinz R, Hammers A, Pavese N, Tai YF*, et al.* Amyloid, hypometabolism, and cognition in Alzheimer disease. Neurology 2007; 68(7): 501.

Esch FS, Keim PS, Beattie EC, Blacher RW, Culwell AR, Oltersdorf T*, et al.* Cleavage of amyloid beta peptide during constitutive processing of its precursor. Science 1990; 248(4959): 1122-4.

Ewers M, Insel P, Jagust WJ, Shaw L, Trojanowski JJ, Aisen P*, et al.* CSF Biomarker and PIB-PET-Derived Beta-Amyloid Signature Predicts Metabolic, Gray Matter, and Cognitive Changes in Nondemented Subjects. Cereb Cortex 2012; 22(9): 1993-2004.

Fantini S, Sassaroli A, Tgavalekos KT, Kornbluth J. Cerebral blood flow and autoregulation: current measurement techniques and prospects for noninvasive optical methods. Neurophotonics 2016; 3(3): 031411-.

Franzmeier N, Duering M, Weiner M, Dichgans M, Ewers M, For the Alzheimer's Disease Neuroimaging I. Left frontal cortex connectivity underlies cognitive reserve in prodromal Alzheimer disease. Neurology 2017; 88(11): 1054-61.

Franzmeier N, Düzel E, Jessen F, Buerger K, Levin J, Duering M*, et al.* Left frontal hub connectivity delays cognitive impairment in autosomal-dominant and sporadic Alzheimer's disease. Brain : a journal of neurology 2018a; 141(4): 1186-200.

Franzmeier N, Hartmann J, Taylor ANW, Araque-Caballero MÁ, Simon-Vermot L, Kambeitz-Ilankovic L*, et al.* The left frontal cortex supports reserve in aging by enhancing functional network efficiency. Alzheimers Res Ther 2018b; 10(1): 28-.

Gevers S, van Osch MJ, Bokkers RPH, Kies DA, Teeuwisse WM, Majoie CB*, et al.* Intra- and multicenter reproducibility of pulsed, continuous and pseudo-continuous arterial spin labeling methods for measuring cerebral perfusion. Journal of cerebral blood flow and metabolism : official journal of the International Society of Cerebral Blood Flow and Metabolism 2011; 31(8): 1706-15.

Giannakopoulos P, Herrmann FR, Bussière T, Bouras C, Kövari E, Perl DP*, et al.* Tangle and neuron numbers, but not amyloid load, predict cognitive status in Alzheimer's disease. Neurology 2003; 60(9): 1495-500.

Gordon BA, McCullough A, Mishra S, Blazey TM, Su Y, Christensen J*, et al.* Cross-sectional and longitudinal atrophy is preferentially associated with tau rather than amyloid beta positron emission tomography pathology. Alzheimer's & dementia (Amsterdam, Netherlands) 2018; 10: 245-52.

Gravina SA, Ho L, Eckman CB, Long KE, Otvos L, Jr., Younkin LH*, et al.* Amyloid beta protein (A beta) in Alzheimer's disease brain. Biochemical and immunocytochemical analysis with antibodies specific for forms ending at A beta 40 or A beta 42(43). J Biol Chem 1995; 270(13): 7013-6.

Gregg NM, Kim AE, Gurol ME, Lopez OL, Aizenstein HJ, Price JC*, et al.* Incidental Cerebral Microbleeds and Cerebral Blood Flow in Elderly Individuals. JAMA Neurol 2015; 72(9): 1021-8.

Gu L, Guo Z. Alzheimer's Aβ42 and Aβ40 peptides form interlaced amyloid fibrils. J Neurochem 2013; 126(3): 305-11.

Habert M-O, de Souza LC, Lamari F, Daragon N, Desarnaud S, Jardel C*, et al.* Brain perfusion SPECT correlates with CSF biomarkers in Alzheimer’s disease. European Journal of Nuclear Medicine and Molecular Imaging 2010; 37(3): 589-93.

Hanseeuw BJ, Betensky RA, Schultz AP, Papp KV, Mormino EC, Sepulcre J*, et al.* Fluorodeoxyglucose metabolism associated with tau-amyloid interaction predicts memory decline. Annals of neurology 2017; 81(4): 583-96.

Hays CC, Zlatar ZZ, Meloy MJ, Osuna J, Liu TT, Galasko DR*, et al.* Anterior Cingulate Structure and Perfusion is Associated with Cerebrospinal Fluid Tau among Cognitively Normal Older Adult APOEvarepsilon4 Carriers. Journal of Alzheimer's disease : JAD 2020; 73(1): 87-101.

Hedden T, Oh H, Younger AP, Patel TA. Meta-analysis of amyloid-cognition relations in cognitively normal older adults. Neurology 2013; 80(14): 1341-8.

Hoenig MC, Bischof GN, Hammes J, Faber J, Fliessbach K, van Eimeren T*, et al.* Tau pathology and cognitive reserve in Alzheimer's disease. Neurobiology of aging 2017; 57: 1-7.

Huber CM, Yee C, May T, Dhanala A, Mitchell CS. Cognitive Decline in Preclinical Alzheimer's Disease: Amyloid-Beta versus Tauopathy. Journal of Alzheimer's disease : JAD 2018; 61(1): 265-81.

Huijbers W, Mormino EC, Wigman SE, Ward AM, Vannini P, McLaren DG*, et al.* Amyloid deposition is linked to aberrant entorhinal activity among cognitively normal older adults. The Journal of neuroscience : the official journal of the Society for Neuroscience 2014; 34(15): 5200-10.

Iaccarino L, Tammewar G, Ayakta N, Baker SL, Bejanin A, Boxer AL*, et al.* Local and distant relationships between amyloid, tau and neurodegeneration in Alzheimer's Disease. NeuroImage: Clinical 2018; 17: 452-64.

Iadecola C. The pathobiology of vascular dementia. Neuron 2013; 80(4): 844-66.

Jack CR, Bennett DA, Blennow K, Carrillo MC, Dunn B, Haeberlein SB*, et al.* NIA-AA Research Framework: Toward a biological definition of Alzheimer's disease. Alzheimer's & Dementia 2018; 14(4): 535-62.

Jack CR, Knopman DS, Jagust WJ, Shaw LM, Aisen PS, Weiner MW*, et al.* Hypothetical model of dynamic biomarkers of the Alzheimer's pathological cascade. Lancet neurology 2010; 9(1): 119.

Johnson NA, Jahng G-H, Weiner MW, Miller BL, Chui HC, Jagust WJ*, et al.* Pattern of cerebral hypoperfusion in Alzheimer disease and mild cognitive impairment measured with arterial spin-labeling MR imaging: initial experience. Radiology 2005; 234(3): 851-9.

Johnson SC, Christian BT, Okonkwo OC, Oh JM, Harding S, Xu G*, et al.* Amyloid burden and neural function in people at risk for Alzheimer's Disease. Neurobiology of aging 2014; 35(3): 576-84.

Kilroy E, Apostolova L, Liu C, Yan L, Ringman J, Wang DJ. Reliability of two-dimensional and three-dimensional pseudo-continuous arterial spin labeling perfusion MRI in elderly populations: comparison with 15O-water positron emission tomography. J Magn Reson Imaging 2014; 39(4): 931-9.

Kim CM, Alvarado RL, Stephens K, Wey HY, Wang DJJ, Leritz EC*, et al.* Associations between cerebral blood flow and structural and functional brain imaging measures in individuals with neuropsychologically defined mild cognitive impairment. Neurobiology of aging 2020; 86: 64-74.

Kim HJ, Park S, Cho H, Jang YK, San Lee J, Jang H*, et al.* Assessment of Extent and Role of Tau in Subcortical Vascular Cognitive Impairment Using 18F-AV1451 Positron Emission Tomography Imaging. JAMA Neurol 2018; 75(8): 999-1007.

Klunk WE, Engler H, Nordberg A, Wang Y, Blomqvist G, Holt DP*, et al.* Imaging brain amyloid in Alzheimer's disease with Pittsburgh Compound-B. Annals of Neurology 2004; 55(3): 306-19.

Kukull WA, Higdon R, Bowen JD, McCormick WC, Teri L, Schellenberg GD*, et al.* Dementia and Alzheimer Disease Incidence: A Prospective Cohort Study. Archives of Neurology 2002; 59(11): 1737-46.

La Joie R, Visani AV, Baker SL, Brown JA, Bourakova V, Cha J*, et al.* Prospective longitudinal atrophy in Alzheimer's disease correlates with the intensity and topography of baseline tau-PET. Science Translational Medicine 2020; 12(524): eaau5732.

Laing KK, Simoes S, Baena-Caldas GP, Lao PJ, Kothiya M, Igwe KC*, et al.* Cerebrovascular disease promotes tau pathology in Alzheimer's disease. Brain Commun 2020; 2(2): fcaa132.

Landau SM, Mintun MA, Joshi AD, Koeppe RA, Petersen RC, Aisen PS*, et al.* Amyloid deposition, hypometabolism, and longitudinal cognitive decline. Annals of neurology 2012; 72(4): 578-86.

Lee VM, Goedert M, Trojanowski JQ. Neurodegenerative tauopathies. Annu Rev Neurosci 2001; 24: 1121-59.

Leijenaar JF, van Maurik IS, Kuijer JPA, van der Flier WM, Scheltens P, Barkhof F*, et al.* Lower cerebral blood flow in subjects with Alzheimer's dementia, mild cognitive impairment, and subjective cognitive decline using two-dimensional phase-contrast magnetic resonance imaging. Alzheimer's & Dementia: Diagnosis, Assessment & Disease Monitoring 2017; 9: 76-83.

Levenga J, Krishnamurthy P, Rajamohamedsait H, Wong H, Franke TF, Cain P*, et al.* Tau pathology induces loss of GABAergic interneurons leading to altered synaptic plasticity and behavioral impairments. Acta Neuropathologica Communications 2013; 1(1): 34.

Li Y, Rinne JO, Mosconi L, Pirraglia E, Rusinek H, DeSanti S*, et al.* Regional analysis of FDG and PIB-PET images in normal aging, mild cognitive impairment, and Alzheimer's disease. Eur J Nucl Med Mol Imaging 2008; 35(12): 2169-81.

Liu TT, Brown GG. Measurement of cerebral perfusion with arterial spin labeling: Part 1. Methods. Journal of the International Neuropsychological Society 2007; 13(3): 517-25.

Lowe VJ, Weigand SD, Senjem ML, Vemuri P, Jordan L, Kantarci K*, et al.* Association of hypometabolism and amyloid levels in aging, normal subjects. Neurology 2014; 82(22): 1959-67.

Maass A, Lockhart SN, Harrison TM, Bell RK, Mellinger T, Swinnerton K*, et al.* Entorhinal Tau Pathology, Episodic Memory Decline, and Neurodegeneration in Aging. The Journal of Neuroscience 2018; 38(3): 530-43.

Mattsson N, Tosun D, Insel PS, Simonson A, Jack CR, Jr., Beckett LA*, et al.* Association of brain amyloid-β with cerebral perfusion and structure in Alzheimer's disease and mild cognitive impairment. Brain : a journal of neurology 2014; 137(Pt 5): 1550-61.

McDade E, Kim A, James J, Sheu LK, Kuan DC-H, Minhas D*, et al.* Cerebral perfusion alterations and cerebral amyloid in autosomal dominant Alzheimer disease. Neurology 2014; 83(8): 710.

Michels L, Warnock G, Buck A, Macauda G, Leh SE, Kaelin AM*, et al.* Arterial spin labeling imaging reveals widespread and Abeta-independent reductions in cerebral blood flow in elderly apolipoprotein epsilon-4 carriers. Journal of cerebral blood flow and metabolism : official journal of the International Society of Cerebral Blood Flow and Metabolism 2016; 36(3): 581-95.

Miller DL, Papayannopoulos IA, Styles J, Bobin SA, Lin YY, Biemann K*, et al.* Peptide compositions of the cerebrovascular and senile plaque core amyloid deposits of Alzheimer's disease. Arch Biochem Biophys 1993; 301(1): 41-52.

Minoshima S, Giordani B, Berent S, Frey KA, Foster NL, Kuhl DE. Metabolic reduction in the posterior cingulate cortex in very early Alzheimer's disease. Annals of Neurology 1997; 42(1): 85-94.

Mosconi L. Brain glucose metabolism in the early and specific diagnosis of Alzheimer’s disease. European Journal of Nuclear Medicine and Molecular Imaging 2005; 32(4): 486-510.

Mosconi L. Glucose metabolism in normal aging and Alzheimer's disease: Methodological and physiological considerations for PET studies. Clinical and translational imaging 2013; 1(4): 10.1007/s40336-013-0026-y.

Mosconi L, De Santi S, Li J, Tsui WH, Li Y, Boppana M*, et al.* Hippocampal hypometabolism predicts cognitive decline from normal aging. Neurobiology of aging 2008; 29(5): 676-92.

Nelson PT, Alafuzoff I, Bigio EH, Bouras C, Braak H, Cairns NJ*, et al.* Correlation of Alzheimer disease neuropathologic changes with cognitive status: a review of the literature. J Neuropathol Exp Neurol 2012; 71(5): 362-81.

Oh H, Habeck C, Madison C, Jagust W. Covarying alterations in Aβ deposition, glucose metabolism, and gray matter volume in cognitively normal elderly. Human brain mapping 2014; 35(1): 10.1002/hbm.22173.

Okamura N, Harada R, Furumoto S, Arai H, Yanai K, Kudo Y. Tau PET Imaging in Alzheimer’s Disease. Current Neurology and Neuroscience Reports 2014; 14(11): 500.

Okonkwo OC, Xu G, Oh JM, Dowling NM, Carlsson CM, Gallagher CL*, et al.* Cerebral blood flow is diminished in asymptomatic middle-aged adults with maternal history of Alzheimer's disease. Cereb Cortex 2014; 24(4): 978-88.

Onkenhout L, Appelmans N, Kappelle LJ, Koek D, Exalto L, de Bresser J*, et al.* Cerebral Perfusion and the Burden of Small Vessel Disease in Patients Referred to a Memory Clinic. Cerebrovascular Diseases 2020; 49(5): 481-6.

Ossenkoppele R, Schonhaut DR, Schöll M, Lockhart SN, Ayakta N, Baker SL*, et al.* Tau PET patterns mirror clinical and neuroanatomical variability in Alzheimer's disease. Brain 2016; 139(5): 1551-67.

Park DC, Reuter-Lorenz P. The adaptive brain: aging and neurocognitive scaffolding. Annu Rev Psychol 2009; 60: 173-96.

Park L, Hochrainer K, Hattori Y, Ahn SJ, Anfray A, Wang G*, et al.* Tau induces PSD95–neuronal NOS uncoupling and neurovascular dysfunction independent of neurodegeneration. Nature Neuroscience 2020; 23(9): 1079-89.

Petersen RC, Aisen PS, Beckett LA, Donohue MC, Gamst AC, Harvey DJ*, et al.* Alzheimer's Disease Neuroimaging Initiative (ADNI): Clinical characterization. Neurology 2010; 74(3): 201-9.

Phelps ME, Huang SC, Hoffman EJ, Selin C, Sokoloff L, Kuhl DE. Tomographic measurement of local cerebral glucose metabolic rate in humans with (F-18)2-fluoro-2-deoxy-D-glucose: validation of method. Ann Neurol 1979; 6(5): 371-88.

Pontecorvo MJ, Devous MD, Kennedy I, Navitsky M, Lu M, Galante N*, et al.* A multicentre longitudinal study of flortaucipir (18F) in normal ageing, mild cognitive impairment and Alzheimer's disease dementia. Brain 2019; 142(6): 1723-35.

Prohovnik I, Mayeux R, Sackeim HA, Smith G, Stern Y, Alderson PO. Cerebral perfusion as a diagnostic marker of early Alzheimer's disease. Neurology 1988; 38(6): 931-7.

Rabinovici GD, Jagust WJ, Furst AJ, Ogar JM, Racine CA, Mormino EC*, et al.* Abeta amyloid and glucose metabolism in three variants of primary progressive aphasia. Annals of neurology 2008; 64(4): 388-401.

Rentz DM, Mormino EC, Papp KV, Betensky RA, Sperling RA, Johnson KA. Cognitive resilience in clinical and preclinical Alzheimer's disease: the Association of Amyloid and Tau Burden on cognitive performance. Brain imaging and behavior 2017; 11(2): 383-90.

Rocher AB, Chapon F, Blaizot X, Baron JC, Chavoix C. Resting-state brain glucose utilization as measured by PET is directly related to regional synaptophysin levels: a study in baboons. NeuroImage 2003; 20(3).

Rubinski A, Franzmeier N, Neitzel J, Ewers M, the Alzheimer's Disease Neuroimaging I. FDG-PET hypermetabolism is associated with higher tau-PET in mild cognitive impairment at low amyloid-PET levels. Alzheimers Res Ther 2020; 12(1): 133.

Schöll M, Lockhart SN, Schonhaut DR, O'Neil JP, Janabi M, Ossenkoppele R*, et al.* PET Imaging of Tau Deposition in the Aging Human Brain. Neuron 2016; 89(5): 971-82.

Selkoe DJ. The cell biology of beta-amyloid precursor protein and presenilin in Alzheimer's disease. Trends Cell Biol 1998; 8(11): 447-53.

Serra L, Mancini M, Cercignani M, Di Domenico C, Spanò B, Giulietti G*, et al.* Network-Based Substrate of Cognitive Reserve in Alzheimer's Disease. Journal of Alzheimer's disease : JAD 2017; 55(1): 421-30.

Shaffer JL, Petrella JR, Sheldon FC, Choudhury KR, Calhoun VD, Coleman RE*, et al.* Predicting cognitive decline in subjects at risk for Alzheimer disease by using combined cerebrospinal fluid, MR imaging, and PET biomarkers. Radiology 2013; 266(2): 583-91.

Shi Y, Thrippleton MJ, Makin SD, Marshall I, Geerlings MI, de Craen AJM*, et al.* Cerebral blood flow in small vessel disease: A systematic review and meta-analysis. Journal of cerebral blood flow and metabolism : official journal of the International Society of Cerebral Blood Flow and Metabolism 2016; 36(10): 1653-67.

Shimojo M, Takuwa H, Takado Y, Tokunaga M, Tsukamoto S, Minatohara K*, et al.* Selective Disruption of Inhibitory Synapses Leading to Neuronal Hyperexcitability at an Early Stage of Tau Pathogenesis in a Mouse Model. The Journal of Neuroscience 2020; 40(17): 3491.

Small GW, Mazziotta JC, Collins MT, Baxter LR, Phelps ME, Mandelkern MA*, et al.* Apolipoprotein E Type 4 Allele and Cerebral Glucose Metabolism in Relatives at Risk for Familial Alzheimer Disease. JAMA 1995; 273(12): 942-7.

Stern Y. What is cognitive reserve? Theory and research application of the reserve concept. J Int Neuropsychol Soc 2002; 8(3): 448-60.

Stern Y. Cognitive reserve. Neuropsychologia 2009; 47(10): 2015-28.

Stern Y. Cognitive reserve in ageing and Alzheimer's disease. Lancet Neurol 2012; 11(11): 1006-12.

Stomrud E, Forsberg A, Hägerström D, Ryding E, Blennow K, Zetterberg H*, et al.* CSF Biomarkers Correlate with Cerebral Blood Flow on SPECT in Healthy Elderly. Dementia and Geriatric Cognitive Disorders 2012; 33(2-3): 156-63.

Tosun D, Joshi S, Weiner MW, the Alzheimer's Disease Neuroimaging I. Multimodal MRI-based Imputation of the Abeta+ in Early Mild Cognitive Impairment. Ann Clin Transl Neurol 2014; 1(3): 160-70.

Trojanowski JQ, Lee VMY. Phosphorylation of paired helical filament tau in Alzheimer's disease neurofibrillary lesions: focusing on phosphatases. The FASEB Journal 1995; 9(15): 1570-6.

Vemuri P, Weigand SD, Przybelski SA, Knopman DS, Smith GE, Trojanowski JQ*, et al.* Cognitive reserve and Alzheimer's disease biomarkers are independent determinants of cognition. Brain 2011; 134(Pt 5): 1479-92.

Villeneuve S, Reed BR, Wirth M, Haase CM, Madison CM, Ayakta N*, et al.* Cortical thickness mediates the effect of β-amyloid on episodic memory. Neurology 2014; 82(9): 761-7.

Whitwell JL, Graff-Radford J, Tosakulwong N, Weigand SD, Machulda MM, Senjem ML*, et al.* Imaging correlations of tau, amyloid, metabolism, and atrophy in typical and atypical Alzheimer's disease. Alzheimer's & Dementia: The Journal of the Alzheimer's Association 2018; 14(8): 1005-14.

Wierenga CE, Clark LR, Dev SI, Shin DD, Jurick SM, Rissman RA*, et al.* Interaction of age and APOE genotype on cerebral blood flow at rest. Journal of Alzheimer's disease : JAD 2013; 34(4): 921-35.

Wierenga CE, Dev SI, Shin DD, Clark LR, Bangen KJ, Jak AJ*, et al.* Effect of mild cognitive impairment and APOE genotype on resting cerebral blood flow and its association with cognition. Journal of cerebral blood flow and metabolism : official journal of the International Society of Cerebral Blood Flow and Metabolism 2012; 32(8): 1589-99.

Wong DF, Rosenberg PB, Zhou Y, Kumar A, Raymont V, Ravert HT*, et al.* In vivo imaging of amyloid deposition in Alzheimer disease using the radioligand 18F-AV-45 (florbetapir [corrected] F 18). Journal of nuclear medicine : official publication, Society of Nuclear Medicine 2010; 51(6): 913-20.

Xia C, Makaretz SJ, Caso C, McGinnis S, Gomperts SN, Sepulcre J*, et al.* Association of In Vivo [18F]AV-1451 Tau PET Imaging Results With Cortical Atrophy and Symptoms in Typical and Atypical Alzheimer Disease. JAMA neurology 2017; 74(4): 427-36.

Xu G, Rowley HA, Wu G, Alsop DC, Shankaranarayanan A, Dowling M*, et al.* Reliability and precision of pseudo-continuous arterial spin labeling perfusion MRI on 3.0 T and comparison with 15O-water PET in elderly subjects at risk for Alzheimer's disease. NMR Biomed 2010; 23(3): 286-93.

Yan L, Liu CY, Wong K-P, Huang S-C, Mack WJ, Jann K*, et al.* Regional association of pCASL-MRI with FDG-PET and PiB-PET in people at risk for autosomal dominant Alzheimer's disease. Neuroimage Clin 2017; 17: 751-60.

Yi D, Lee DY, Sohn BK, Choe YM, Seo EH, Byun MS*, et al.* Beta-Amyloid Associated Differential Effects of APOE ε4 on Brain Metabolism in Cognitively Normal Elderly. The American Journal of Geriatric Psychiatry 2014; 22(10): 961-70.

Young PNE, Estarellas M, Coomans E, Srikrishna M, Beaumont H, Maass A*, et al.* Imaging biomarkers in neurodegeneration: current and future practices. Alzheimers Res Ther 2020; 12(1): 49.

Manuscript 1

Rubinski, A., Franzmeier, N., Neitzel, J., & Ewers, M. (2020). FDG-PET hypermetabolism is associated with higher tau-PET in mild cognitive impairment at low amyloid-PET levels. *Alzheimer's research & therapy, 12*(1), 1-12.

DOI: 10.1186/s13195-020-00702-6.

Contributions: AR is the first author on this manuscript, AR processed the data, conducted the analyses, interpreted the results, and wrote the manuscript, NF and JN provided critical review of the manuscript, and ME designed the study, interpreted the results, and wrote the manuscript.

Rubinski et al. Alzheimer's Research & Therapy (2020) 12:133
https://doi.org/10.1186/s13195-020-00702-6

Alzheimer's Research & Therapy

RESEARCH Open Access

FDG-PET hypermetabolism is associated with higher tau-PET in mild cognitive impairment at low amyloid-PET levels

Anna Rubinski[1], Nicolai Franzmeier[1], Julia Neitzel[1], Michael Ewers[1,2*] and the Alzheimer's Disease Neuroimaging Initiative (ADNI)

Abstract

Background: FDG-PET hypermetabolism can be observed in mild cognitive impairment (MCI), but the link to primary pathologies of Alzheimer's diseases (AD) including amyloid and tau is unclear.

Methods: Using voxel-based regression, we assessed local interactions between amyloid- and tau-PET on spatially matched FDG-PET in 72 MCI patients. Control groups included cerebrospinal fluid biomarker characterized cognitively normal (CN, $n = 70$) and AD dementia subjects ($n = 95$).

Results: In MCI, significant amyloid-PET by tau-PET interactions were found in frontal, lateral temporal, and posterior parietal regions, where higher local tau-PET was associated with higher spatially corresponding FDG-PET at low levels of local amyloid-PET. FDG-PET in brain regions with a significant local amyloid- by tau-PET interaction was higher compared to that in CN and AD dementia and associated with lower episodic memory.

Conclusion: Higher tau-PET in the presence of low amyloid-PET is associated with abnormally increased glucose metabolism that is accompanied by episodic memory impairment.

Keywords: FDG-PET, Hypermetabolism, Tau-PET, Amyloid-PET, Hyperactivation, Mild cognitive impairment

Introduction

In Alzheimer's disease (AD), alterations in glucose metabolism as assessed by [^{18}F]fluorodeoxyglucose positron emission tomography (FDG-PET) are a common pathological hallmark [1]. Specifically, FDG-PET hypometabolism within temporoparietal regions is commonly observed in AD dementia and earlier AD stages, including in amyloid-positive mild cognitive impairment (MCI; i.e., prodromal AD) [2] and cognitively normal (CN) elderly at genetic risk of AD [3]. However, FDG-PET metabolism shows complex changes during the course of AD, where not only reductions but also increases in FDG-PET metabolism have been reported across CN amyloid-positive subjects [4] and subjects at genetic risk of AD [5, 6] and MCI [7]. Thus, clinical staging of cognitive symptoms does not correspond to FDG-PET alterations in a straightforward manner.

Studies using amyloid- and tau-PET imaging suggest that these pathologies are important predictors of regional FDG-PET alterations. For amyloid-PET, elevated global levels of amyloid-PET have been associated with reduced FDG-PET in both AD dementia [8] and MCI [9]. However, increased FDG-PET has also been observed in association with elevated amyloid-PET [4]. Furthermore, there is a poor regional match between amyloid-PET and FDG-PET in typical [10] and atypical AD [11] suggesting that amyloid-PET alone cannot fully

* Correspondence: Michael.Ewers@med.uni-muenchen.de
[1]Institute for Stroke and Dementia Research, Klinikum der Universität München, Ludwig-Maximilians-Universität LMU, Feodor-Lynen-Straße 17, 81377 Munich, Germany
[2]German Center for Neurodegenerative Diseases, Munich, Germany

account for FDG-PET alterations. Results from tau-PET studies suggest that tau pathology may be an important modulating factor of FDG-PET [12–14]. Results from recent studies in elderly asymptomatic CN revealed an interaction between amyloid- and tau-PET, where higher tau-PET was associated with *higher* FDG-PET at low levels of amyloid-PET, but with lower levels of FDG-PET at high levels of amyloid-PET [15, 16]. These results provide an intriguing model of the dynamic bidirectional changes in relationship to beta-amyloid (Aβ) and tau pathology. The focus on biomarkers of Aβ and tau pathology rather than the clinical diagnosis of AD allows to investigate the effect of different mixtures of both pathologies on FDG-PET changes and cognitive impairment. This is important because even in the absence of abnormal levels of Aβ, abnormal tau-PET levels can be observed in higher cortical brain areas in a substantial number of elderly subjects, where higher tau-PET was associated with cognitive impairment [17]. However, the association of higher tau-PET with FDG-PET alterations at varying levels of Aβ in symptomatic elderly subjects is unclear. In order to address this research gap, we examined both the main and interaction effects of [^{18}F]AV45 amyloid-PET and [^{18}F]AV1451 tau-PET on FDG-PET in subjects with amnestic MCI. Furthermore, we tested whether the observed higher levels of FDG-PET represent abnormally increased FDG-PET, i.e., FDG-PET hypermetabolism, and whether such increases in FDG-PET are beneficial or detrimental for cognition.

Methods

Participants

All subjects were recruited within the Alzheimer's Disease Neuroimaging Initiative (ADNI phase III; http://adni.loni.usc.edu/) [18]. Inclusion criteria for the current study beyond those of ADNI were a diagnosis of MCI at the PET acquisition visit (Mini-Mental State Examination (MMSE) > 24, Clinical Dementia Rating (CDR) = 0.5, objective memory loss on the education-adjusted Wechsler Memory Scale II, preserved activities of daily living) and the availability of [^{18}F]AV1451 tau-PET, [^{18}F]AV45 amyloid-PET, and [^{18}F]FDG-PET up to 6 months apart. From the total sample of 74 MCI subjects fulfilling the inclusion criteria, two subjects failed preprocessing and were excluded, yielding a final sample of 72 MCI subjects. Apolipoprotein E (APOE) genotyping was available as well.

In addition to the MCI group with all three PET modalities, a group of 70 cerebrospinal fluid (CSF) Aβ- and p-tau$_{181}$-negative CN subjects (MMSE > 24, CDR = 0) and 95 AD dementia subjects (MMSE < 26, CDR > 0.5, fulfillment of NINCDS/ADRDA criteria for probable AD) [19] were also included to assess group-level differences in regional FDG measures. These subjects were recruited in ADNI phase II and were selected for the current study based on the availability of FDG-PET and CSF biomarkers of Aβ and tau. CN subjects were asymptomatic and Aβ and phosphorylated tau (p-tau) negative based on a quantitative CSF threshold (Elecsys CSF immunoassay; $A\beta_{1-42} > 976.6$ pg/ml, p-tau$_{181} < 21.8$ pg/ml [20];). AD dementia subjects were diagnosed based on ADNI diagnostic criteria and were CSF biomarker positive (Elecsys CSF immunoassay; $A\beta_{1-42} < 976.6$ pg/ml, p-tau$_{181} > 21.8$ pg/ml [20]).

MRI and PET acquisition

All MRI data were obtained on 3-T scanner systems at each ADNI site according to standardized protocol. Tau-PET data were acquired for 30-min dynamic emission scan, six 5-min frames, 75–105 min post-injection of 10.0 mCi of [^{18}F]AV1451. Amyloid-PET data were acquired for 20-min dynamic emission scan, four 5-min frames, 50–70 min post-injection of 10.0 mCi of [^{18}F]AV45. FDG-PET data were acquired for 30-min dynamic emission scan, six 5-min frames, 30–60 min post-injection of 5.0 mCi of [^{18}F]FDG. PET data underwent extensive quality control protocols and standardized image preprocessing correction steps to produce uniform data across the ADNI centers. These steps included frame co-registration, averaging across the dynamic range, and standardization with respect to the orientation, voxel size, and intensity [21]. Detailed information on the imaging protocols and standardized image preprocessing steps for MRI and PET can be found at http://adni.loni.usc.edu/methods.

MRI and PET preprocessing

T1 MRI images acquired in closest temporal proximity to the tau-PET scan were preprocessed using the same SPM12-based (Wellcome Trust Centre for Neuroimaging, University College London) pipeline as described previously [18]. Briefly, for each subject, the T1 MRI image was segmented into gray matter (GM), white matter (WM), and CSF maps. Next, non-linear high-dimensional spatial normalization parameters were estimated, and a group-specific template was created using SPM's DARTEL toolbox. The group-specific template was linearly registered to the MNI template in order to estimate the affine transformation parameters.

For each subject, tau-PET, amyloid-PET, and FDG-PET images were coregistered to the participant's T1 MRI image in native space. For the voxel-based analyses, all PET images were subsequently spatially warped to MNI space using the DARTEL flow fields and affine transformation parameters estimated based on the MRI spatial registration described above. For all PET modalities, standardized uptake value ratio (SUVR) images were computed using the inferior cerebellar gray for tau-

PET, the whole cerebellum for amyloid-PET, or the pons for FDG-PET as reference regions. A GM mask was created by warping the group-average GM map from the DARTEL template to MNI space and binarizing the image to only include voxels that had at least 30% GM probability. We further excluded subcortical structures (basal ganglia, thalamus, cerebellum, and brain stem) from the mask because they were either used as reference region or in order to avoid inclusion of regions that show off-target [^{18}F]AV1451 binding likely unrelated to tau [22]. All PET images were GM masked and smoothed using an 8-mm Gaussian smoothing kernel.

Creation of *z*-transformed deviation images (*z*-maps)

To assess differences in tau deposition, we computed voxel-wise mean and standard deviation of SUVR values for CN. The CN group was recruited in ADNI phase III and consisted of 27 amyloid-negative CN subjects with [^{18}F]AV1451 tau-PET. *z*-score deviation maps were created for each of the MCI subjects, by subtracting from each voxel the voxel-wise mean and dividing by the standard deviation of CN group SUVR.

Assessment of amyloid status

Amyloid status was computed using a pre-established protocol [23]. Specifically, T1 MRI images were segmented and parcellated into cortical regions with Freesurfer (v5.3; surfer.nmr.mgh.harvard.edu/), which was used to extract mean amyloid-PET uptake from GM regions (frontal, lateral temporal, lateral parietal, and anterior/posterior cingulate) relative to the whole cerebellum. Participants were classified as amyloid-positive or amyloid-negative based on established cut-points (global amyloid-PET SUVR ≥ 1.11) [23].

Cognitive assessment

To estimate memory performance, we used ADNI-MEM, an episodic memory composite score based on a broad battery of neuropsychological memory tests [24]. The ADNI-MEM score includes the Rey Auditory Verbal Learning Test, the Alzheimer's Disease Assessment Scale, the Wechsler Logical Memory I and II, and the word recall of the MMSE.

Statistical analysis

Demographics were compared between diagnostic groups using *t* tests for continuous variables and chi-squared tests for categorical variables.

We conducted voxel-based linear regression analyses to test the main effect as well as the local interactions amyloid- by tau-PET on FDG-PET. All analyses were controlled for age, gender, education, study site, and - in case of testing the interaction effect - the main effects of amyloid- and tau-PET. All PET measures were included as continuous variables and obtained in spatially corresponding voxels across all three PET modalities, thus assessing the local relationship between the variables. These calculations were done via the software package VoxelStats, a MATLAB (Mathworks Inc., Natick, MA, USA)-based package for multimodal voxel-wise brain image analysis [25]. The customized GM mask (see above) was used to constrain the analysis to cortical GM. The voxel-based statistical parametric maps were corrected for multiple comparisons, where the statistical significance was defined using a random field theory-based [26] threshold of $p < 0.05$ with a cluster forming threshold of $p < 0.001$. In order to examine the nature of the amyloid- by tau-PET interaction, significant voxel clusters of the interactions were identified and labeled according to the largest overlap to the automated anatomical labeling regions. For all three PET modalities, we extracted the mean voxel values within each cluster showing significant amyloid- by tau-PET interactions on FDG-PET resulting from the voxel-wise analyses. We plotted the interactions to ensure that results were not driven by extreme values. The robustness of the interaction effect for each cluster was tested by rerunning the regression model after removing influential cases defined by Cook's distance *D* [27]. Observations with large influence (the threshold for considering an observation as influential was defined as 4/number of observations) and observations exceeding 3 standard deviations from the mean were excluded in order to test whether the regression coefficient remained significant. Clusters were considered significant and stable when meeting an alpha threshold of 0.05 after removing influential cases.

In addition, post hoc interaction analyses on the mean cluster values were conducted controlling additionally for APOE genotype status (APOE ε4 allele carriers vs non-carriers).

Group-level differences in regional FDG measures were assessed by a one-way ANCOVA (controlling for age, gender, education, and study site) with post hoc *t* test between each pair to assess the difference between MCI subgroups and control groups.

In order to test whether FDG-PET cluster values were associated with memory performance, we conducted for each cluster a linear regression analysis including ADNI-MEM scores as the dependent variable and the FDG-PET cluster values as the predictor, controlling for age, gender, education, and study site.

All statistical analyses were performed using R-statistical software (http://www.R-project.org). Associations were considered significant when meeting an alpha threshold of 0.05.

Results

Sample characteristics

Demographic characteristics and group differences are presented in Table 1. Figure 1 shows the tau-PET

Table 1 Group characteristics (mean ± SD)

	CN ($n = 70$)	MCI ($n = 72$)	AD dementia ($n = 95$)
Age (years)	72.00 ± 5.48[c]	76.74 ± 7.33	74.11 ± 8.60[a]
Gender (M/F)	33/37	42/30	52/44
Education (years)	16.53 ± 2.65	16.33 ± 2.88	15.48 ± 2.68
MMSE	28.99 ± 1.22[b]	28.22 ± 1.88	22.98 ± 2.04[c]
Aβ−/Aβ+[d]	70/0	42/30	0/95

Abbreviations: *Aβ* amyloid-beta, *AD* Alzheimer's disease, *CN* cognitively normal, *F* female, *M* male, *MCI* mild cognitive impairment, *MMSE* Mini-Mental State Exam
Significantly different from MCI—[a]$p < 0.05$, [b]$p < 0.01$, and [c]$p < 0.001$
[d]Aβ status was determined via PET in MCI and via CSF in CN and AD dementia groups

distribution within amyloid-negative CN subjects. Tau-PET levels predominantly in the temporal lobe were higher in MCI compared to those in amyloid-negative CN (Fig. 1b).

Voxel-wise amyloid- and tau-PET main effects on FDG-PET metabolism

First, we tested the main effects of amyloid- and tau-PET on FDG-PET in MCI. As shown in Fig. 2 (for statistics, see supplementary Table 1), higher amyloid-PET was associated with higher FDG-PET in small clusters located in the right superior frontal, right occipital, left cuneus, and right temporal pole. On the other hand, higher tau-PET was associated with higher FDG-PET in multiple regions within the bilateral parietal lobe, left insular, and cingulate cortices. Negative associations were primarily observed within the left middle frontal and left temporoparietal regions.

When stratified by amyloid status (global amyloid-PET SUVR ≥ 1.11), the associations between higher tau-PET and higher FDG-PET metabolism are evident only within the amyloid-negative subgroup, while the opposite association was primarily observed in the amyloid-positive subgroup (Fig. 2, Table 1).

Voxel-wise amyloid- by tau-PET interactions on FDG-PET metabolism

Since we found that the associations between tau-PET and FDG-PET are dependent on Aβ levels, we further tested the local amyloid- by tau-PET interaction on FDG-PET in MCI. Linear regression analysis of the interaction of amyloid-PET by tau-PET (included as continuous variables) showed significant effects in multiple brain regions. In order to examine whether any outliers may drive these interactions, we extracted the mean voxel values in each cluster and examined the undue influence of any observations based on Cook's distance. Those clusters that survived the quality check are displayed in Fig. 3a (for statistics, see Table 2).

All amyloid-PET by tau-PET interactions were of the same direction, i.e., higher tau-PET was associated with higher FDG-PET at low levels of amyloid-PET but not at high levels of amyloid-PET (Fig. 3b). These clusters were predominantly located within the left middle temporal gyrus, right inferior temporal gyrus, right lingual gyrus, left precuneus, bilateral inferior parietal gyrus, left superior frontal gyrus, and right middle frontal gyrus.

To determine whether these effects were driven by differences in *APOE* status, we tested whether *APOE* status had influenced the results. When controlling all above listed models for *APOE*, the observed interactions remained significant ($p < 0.05$) in all clusters.

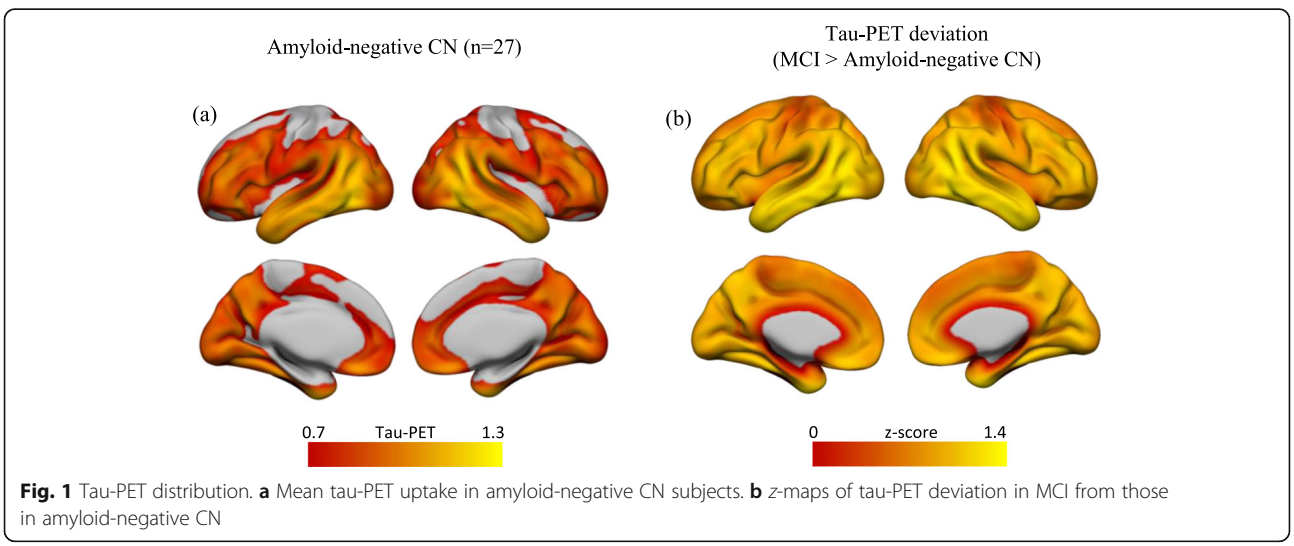

Fig. 1 Tau-PET distribution. **a** Mean tau-PET uptake in amyloid-negative CN subjects. **b** *z*-maps of tau-PET deviation in MCI from those in amyloid-negative CN

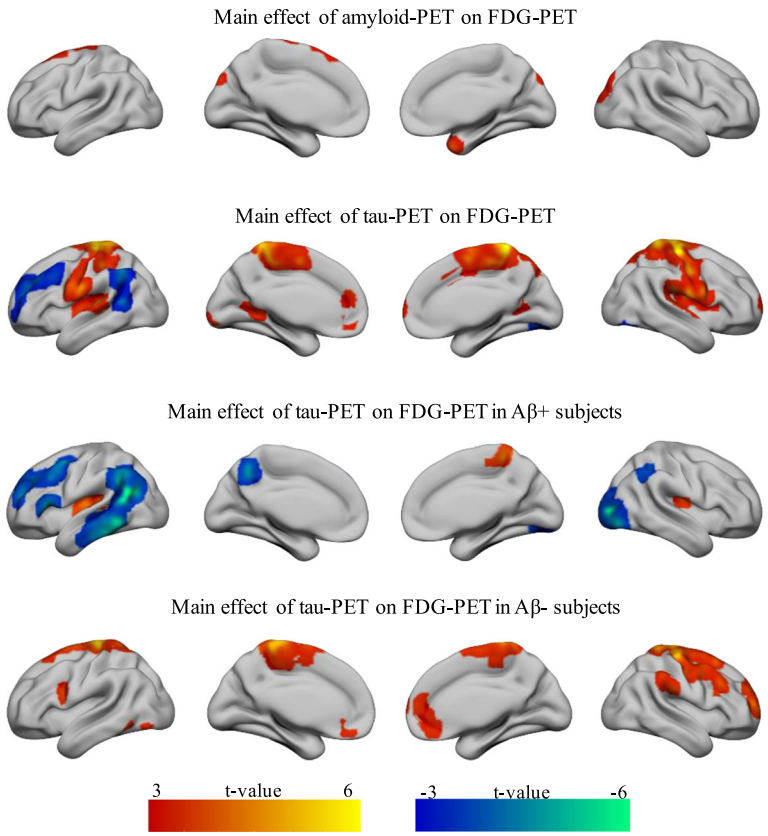

Fig. 2 Main effect of amyloid- and tau-PET on FDG-PET metabolism in MCI. Projection of significant clusters resulting from the voxel-wise analysis. MNI coordinates and *t* values of the peaks are provided in supplementary Table 1

Tau-related hypermetabolism in amyloid-negative MCI subjects

In order to examine whether the observed tau-related increase in FDG-PET cluster values in the MCI subjects with low amyloid represented abnormal FDG-PET *hyper*metabolism, we compared the FDG-PET cluster values in the MCI subgroups to the FDG-PET in amyloid-negative CN ($n = 70$) and subjects with full-blown AD dementia ($n = 95$). Note that these two reference groups including CN and AD dementia were characterized by CSF biomarker profile of $A\beta_{1-42}$ and p-tau_{181} rather than amyloid- and tau-PET given that those imaging modalities were not available in a sufficiently large number of CN and AD dementia subjects.

MCI subjects were divided by high and low tau-PET (median split) and by amyloid status (global amyloid-PET SUVR ≥ 1.11), resulting in four subgroups (high vs low tau/positive vs negative amyloid). FDG-PET levels for all MCI subgroups along with the control groups are plotted in Fig. 4. ANCOVA showed significant ($p < 0.05$) group differences in FDG-PET for all clusters except for one cluster within the left superior frontal gyrus ($p = 0.067$). Post hoc analyses confirmed that the tau-related increase in FDG-PET in the high-tau/amyloid-negative MCI subgroup was significantly higher compared to the CN group in clusters located within the right middle frontal, left middle temporal, and right lingual gyri. The same group also had significantly higher FDG-PET levels compared to AD dementia cases within the same clusters, confirming that the FDG-PET levels will eventually decrease with clinical AD progression.

Hypermetabolism in the right middle frontal cortex is associated with lower memory performance

Next, we addressed the question whether tau-related FDG-PET hypermetabolism in MCI is associated with memory performance. Since FDG-PET hypermetabolism was observed at lower levels of amyloid-PET (see above), we chose to test FDG-PET cluster values as predictors of memory performance in amyloid-negative MCI subjects in each cluster. We found a significant association in the right middle frontal ($p = 0.013$; Fig. 5). The association was negative, meaning higher FDG-PET metabolism in the middle frontal gyrus cluster of FDG-PET

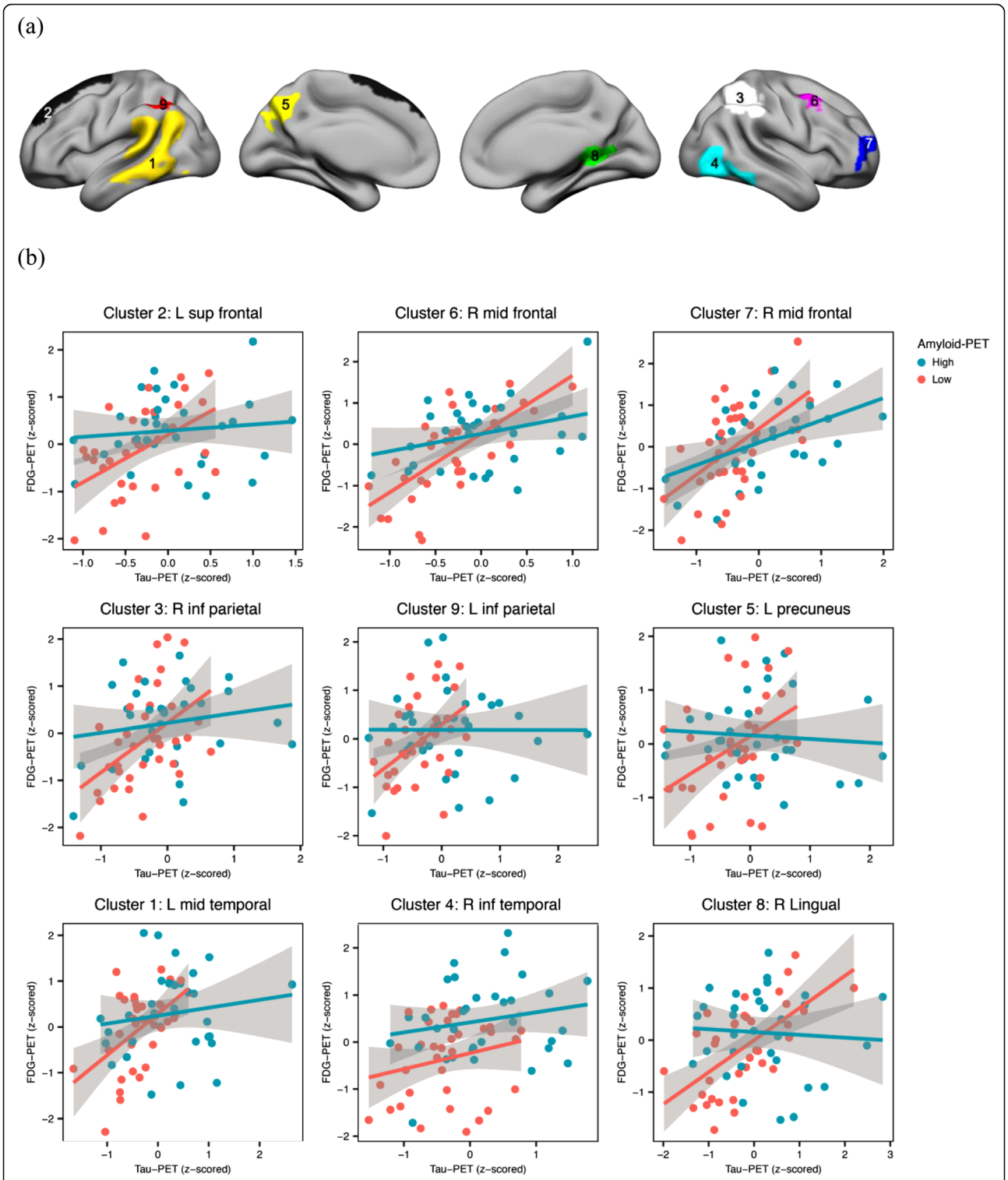

Fig. 3 Regional interactions between amyloid- and tau-PET on FDG-PET metabolism in MCI. **a** Projection of significant clusters resulting from the voxel-wise analysis. **b** Scatterplots are based on mean SUVR values extracted from voxel-wise analyses for each of the significant clusters (arranged by anatomical adjacency). For all statistical analyses, amyloid-PET was used as a continuous measure; for illustrational purposes, however, amyloid levels were binarized into high and low levels (median split). Scatterplots are presented after removal of outliers (i.e., defined as influential observations by Cook's distance and 3 standard deviations from the mean); for regression plots including the outliers, see supplementary Fig. 1

Table 2 Areas showing significant voxel-wise interaction between amyloid- and tau-PET on FDG-PET in MCI

Labels	Cluster index	Size (voxels)	*t* value	MNI coordinates		
				x	*Y*	*z*
L middle temporal	1	3552	5.64	− 51	− 60	24
L superior frontal	2	1853	6.4	− 7.5	27	63
R inferior parietal	3	1448	6.11	52.5	− 36	51
R inferior temporal	4	1122	5.29	58.5	− 49.5	− 24
L precuneus	5	606	5.91	− 4.5	− 76.5	39
R middle frontal	6	444	6.24	37.5	10.5	61.5
R middle frontal	7	432	5.07	36	57	13.5
R lingual	8	224	4.39	21	− 48	6
L inferior parietal	9	191	4.25	− 45	− 51	52.5

L left, *R* right
MNI coordinates and *t* values of the peaks are provided. *t* values are based on voxel-wise regressions controlling for age, gender, education, and study site.

hypermetabolism was associated with a lower ADNI-MEM score. This result suggests that right frontal FDG-PET hypermetabolism is associated with worse memory performance. Control analysis in the amyloid-positive MCI subjects did not show significant associations between FDG-PET and cognition for any of the clusters.

Discussion

Our first major finding showed that higher tau-PET was associated with higher glucose metabolism in subjects with lower levels of amyloid-PET, but not higher levels of amyloid-PET. These effects were predominantly found within the middle temporal gyrus, posterior parietal, and frontal cortex and were independent of APOE genotype. Our second major finding was that the tau-related increases in FDG-PET represented hypermetabolism since the FDG-PET level exceeded that of CN and AD dementia subjects. Our third major finding was that the tau-related FDG-PET hypermetabolism in MCI subjects with low amyloid was associated with lower memory performance.

Our findings advance the current understanding of FDG-PET changes in MCI, providing an explanatory model of FDG-PET hypermetabolism that has been observed in multiple studies in asymptomatic and symptomatic elderly subjects (for a review, see [28]). In line with our results, a recent study in MCI reported increased FDG-PET metabolism at low levels of amyloid-PET but not high levels of amyloid-PET [7]. FDG-PET metabolism was positively associated with Aβ in MCI, but inversely associated with Aβ in AD dementia [29]. We show that tau-PET plays an important role in FDG-PET hypermetabolism in MCI subjects at low Aβ levels, suggesting the interaction of tau and amyloid pathology in non-demented subjects to be key for the increase in FDG-PET. Compared to the interaction approach, our analysis of tau-PET stratified by negative vs positive amyloid-PET showed a more widespread association of higher tau-PET and FDG-PET. Higher tau-PET was preferentially associated with higher FDG-PET in Aβ-negative MCI subjects, but with lower FDG-PET in Aβ-positive subjects, consistent with the results of our interaction analyses. The spatially more restricted interaction effect is probably due to lower statistical power to test an interaction effect compared to testing a main effect.

Our results are consistent with recent findings in CN, where higher tau-PET was associated with higher FDG-PET in participants with low levels of amyloid-PET [15, 16]. We expand significantly above those previous results by showing that the interaction extends to MCI, where the tau-related increase in FDG-PET represents hypermetabolism above normal levels and is associated with lower memory performance. These findings on FDG-PET show parallels to fMRI detected hyperactivation as a function of tau and amyloid pathology. Both resting-state and task-evoked hyperactivity, especially in the medial temporal lobe [30], but also other brain regions [31] has been observed in early-phase autosomal dominant AD [32] and MCI [30, 31, 33]. fMRI-assessed hyperactivation in the medial temporal lobe was associated with faster cognitive decline in MCI [33], consistent with our findings of FDG-PET hypermetabolism to be associated with lower cognitive performance in MCI. Furthermore, fMRI-assessed hyperactivation was associated with higher tau-PET in CN [34, 35]. An interaction of tau-PET by amyloid-PET on resting-state fMRI-assessed network connectivity in CN was observed, such that after a phase of hyperconnectivity, there was a decline in network connectivity when both tau-PET and amyloid-PET were high [36]. These results are reminiscent of the interaction effect of tau-PET by amyloid-PET on FDG-PET observed in the current study. Together, these studies suggest a synergistic interaction of tau and amyloid pathology on brain activity assessed across different modalities.

In the current study, we took a biomarker-centered approach using amyloid- and tau-PET to predict changes in FDG-PET in MCI. A subset of the MCI patients showed no abnormal Aβ levels. Higher tau-PET levels in the absence of abnormal Aβ levels may be due to primary age-related tauopathy (PART) [37]. PART is characterized by elevated tau pathologies confined to Braak-stage regions I–IV at absent or low levels of amyloid plaques and has been proposed to be an etiological entity that is qualitatively different from AD [37, 38]. Although it is still debated whether PART is part of the AD continuum [39], it is generally accepted that abnormal Aβ levels are a defining feature of AD. Thus,

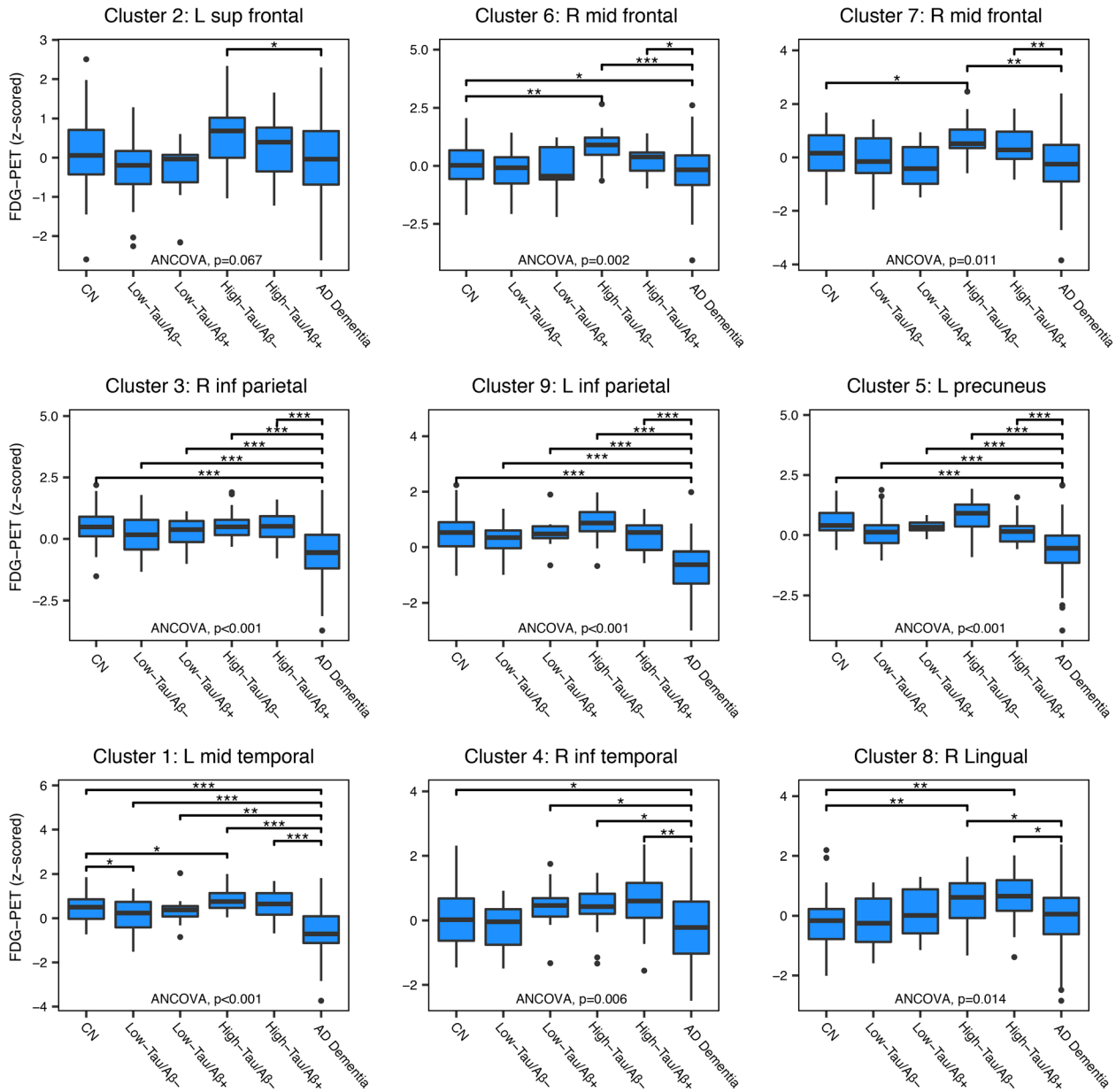

Fig. 4 FDG-PET levels in MCI subgroups compared to CN and AD control groups. Mean FDG-PET levels for each cluster (arranged by anatomical adjacency) compared to CN and AD dementia subjects. MCI subjects were stratified by high and low tau PET (median split) and amyloid PET (global amyloid-PET SUVR ≥ 1.11). Significant differences between groups are indicated by *$p < 0.05$, **$p < 0.01$, and ***$p < 0.001$; one-way ANCOVA with post hoc *t* test between each pair

not all MCI participants were within the AD continuum. Nevertheless, based on biomarker-driven rather than diagnostic characterization, our study showed that the interaction between both types of AD pathologies is predictive of FDG-PET alterations.

The mechanism by which pathologic tau or amyloid is associated with an increase in glucose metabolism remains an open question. In vitro electrophysiological analysis showed that secreted extracellular tau fragments obtained post-mortem from the brain of an individual with AD cause neuronal hyperactivity in human neurons [40]. Moreover, transgenic mice studies showed that reducing tau protein levels in the brain is associated with reduced susceptibility to neuronal hyperexcitability and seizures [41], suggesting that tau modulates neuronal hyperactivity of neuronal networks [42]. The disruption

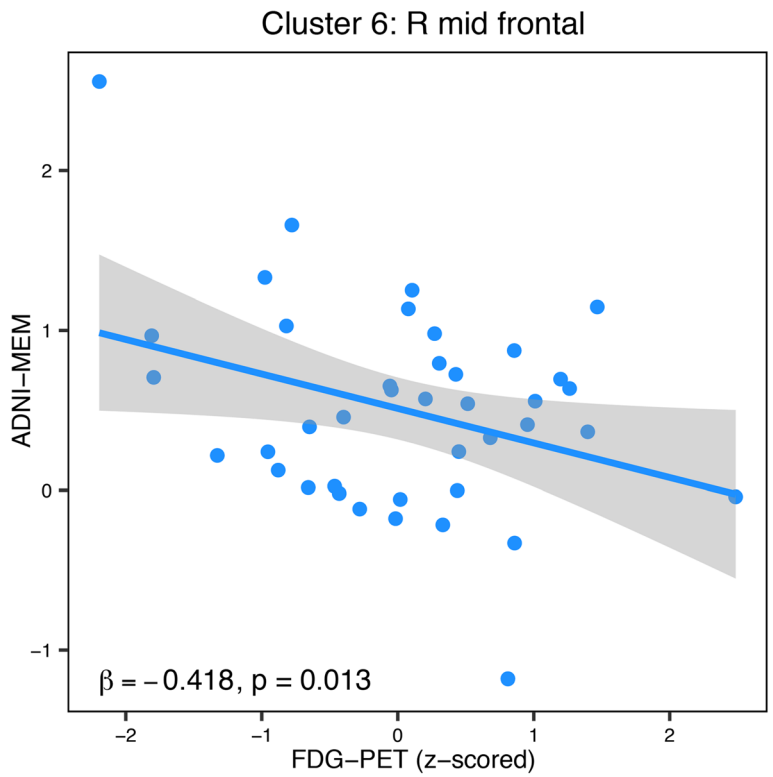

Fig. 5 Associations among FDG-PET and memory performance. Scatterplot for the regression model of FDG-PET on ADNI-MEM in amyloid-negative MCI subjects

of GABAergic neuronal network has been suggested as a possible mechanism of tau-associated disturbance of hippocampal neuron excitability [43]. The differential role of tau and amyloid in driving hypermetabolism is somewhat unclear. In transgenic mice expressing amyloid, higher amyloid was linked to higher neural excitability [44]. A recent study in transgenic mouse models of tau and amyloid suggests that amyloid is driving neuronal hyperactivity, but increased levels of tau lead to reduced neuronal activity [45]. However, these results are in conflict with previous results of the amyloid-independent association of tau-related susceptibility to hyperexcitability discussed above [41]. One possibility to reconcile the findings is that tau enhances amyloid-related neuronal hyperactivity at lower levels of amyloid, but reduces neuronal function at higher levels of amyloid. This stance would be in agreement with results from previous studies in humans reporting tau-PET but not amyloid-PET to be linked to fMRI-assessed hyperactivation [35] or FDG-PET hypermetabolism [15, 16]. Furthermore, we observed FDG-PET hypermetabolism in the group of amyloid-negative/high-tau but not amyloid-positive/low-tau suggesting that higher levels of tau in the presence of lower levels of amyloid are decisive for FDG-PET hypermetabolism. As a third alternative, neuronal hyperexcitability may drive initial tau release, propagation, and spread [46, 47]. Future preclinical and intervention studies targeting amyloid or tau pathology will be instrumental in disentangling the causative relationship between primary AD pathologies and FDG-PET hypermetabolism.

Another major finding of our study was the association between FDG-PET hypermetabolism and lower memory performance suggesting that FDG-PET hypermetabolism may reflect pathologically altered FDG-PET levels that are detrimental rather than of compensatory nature. In previous studies including cognitively impaired elderly subjects, increased FDG-PET in the hippocampal formation was associated with poorer cognitive performance [48]. Moreover, reducing hippocampal hyperactivity by drug intervention improves cognition in MCI [49], where the same drug reduced tau-related neuronal hyperexcitability in a transgenic mouse model of AD [50]. Alternatively, higher neural activity may enhance tau spreading which in turn may lead to cognitive decline [46, 47]. To test such a potentially mutually reinforcing chain of events would require longitudinal studies. With the caution that the current study does not allow for a causative interpretation, our

findings suggest that local FDG-PET hypermetabolism in the presence of tau has no beneficial effect on cognition. We further caution that the MCI syndrome may have been also caused by other pathologies than amyloid and tau pathologies, especially in the MCI subjects with low amyloid. Alternative pathologies that have been linked to AD-like symptoms include cerebrovascular disease, aggregation of the transactive response DNA binding protein 43 kDa (TDP-43), and alpha-synuclein [51–54].

Several caveats need to be considered when interpreting the results of the current study. First, the current study is cross-sectional in nature. A longitudinal study will be informative to test the predictive value of tau- and amyloid-PET for the subsequent changes in FDG-PET and cognition. Second, the presence of the APOE ε4 allele has been previously shown to be associated with glucose hypermetabolism [6] and thus may provide a confounding variable. However, a post hoc analysis showed that the observed interaction remained significant even when controlling for APOE genotype, suggesting that any association between APOE and tau pathology did not explain the current results. Third, although FDG-PET is commonly interpreted to reflect neural activity, it is possible that FDG-PET also reflects glial activity. For example, microglia activation is increased in relation to tau and amyloid pathology and can be associated with FDG-PET hypermetabolism as suggested by findings in mice [55]. However, our results on FDG-PET show parallels with the findings on resting-state and task-evoked fMRI BOLD signal which is less likely to reflect glia activity, discounting the possibility of glia activation as a major source of PET. Fourth, we did not apply partial volume correction to FDG-PET. We did so deliberately in order to avoid that FDG-PET hypermetabolism may occur due to the correction procedure. Here, we observed increased FDG-PET despite not correcting, supporting the view that a true increase in FDG-PET can be observed as a function of tau and amyloid pathology.

Conclusions

We found that FDG-PET hypermetabolism occurs as a function of increased tau-PET in the presence of low amyloid-PET, and is associated with worse cognitive performance. Our results have implications for clinical trials, where FDG-PET is often used as an outcome parameter [56]. Given the non-linear changes of FDG-PET as a function of tau and amyloid pathology, a beneficial drug effect on FDG-PET may not always translate into a reduction in the decline of FDG-PET, but could also be a reduction of the detrimental increase in FDG-PET. Clearly, our results call for a more sophisticated model of FDG-PET changes in the course of AD, taking both amyloid- and tau-PET into account.

Supplementary information

Supplementary information accompanies this paper at https://doi.org/10.1186/s13195-020-00702-6.

Additional file 1: Figure S1. Regional interactions between amyloid- and tau-PET on FDG-PET metabolism in MCI. **Table S1.** Areas showing significant voxel-wise effect of amyloid-PET and tau-PET on FDG-PET in MCI.

Abbreviations

AD: Alzheimer's disease; ADNI: Alzheimer's Disease Neuroimaging Initiative; APOE: Apolipoprotein E; Aβ: Beta-amyloid; CN: Cognitively normal; CSF: Cerebrospinal fluid; FDG: Fluorodeoxyglucose; GM: Gray matter; MCI: Mild cognitive impairment; MMSE: Mini-Mental State Examination; MRI: Magnetic resonance imaging; PET: Positron emission tomography; SUVR: Standard uptake value ratio; WM: White matter

Acknowledgements

Data used in the preparation of this article were obtained from the Alzheimer's Disease Neuroimaging Initiative (ADNI) database (adni.loni.usc.edu). As such, the investigators within the ADNI contributed to the design and implementation of ADNI and/or provided data but did not participate in the analysis or writing of this report. A complete list of ADNI investigators can be found at https://adni.loni.usc.edu/wp-content/uploads/how_to_apply/ADNI_Acknowledgement_List.pdf.

Authors' contributions

AR conducted the analyses and wrote the manuscript, NF and JN provided critical review of the manuscript, and ME designed the study, interpreted the results, and wrote the manuscript. The authors read and approved the final manuscript.

Funding

The work was supported by the LMUexcellent Initiative (to ME) and DFG (German Research Foundation, INST 409/193-1 FUGG). ADNI data collection and sharing for this project was funded by the ADNI (National Institutes of Health Grant U01 AG024904) and DOD ADNI (Department of Defense award number W81XWH-12-2-0012). ADNI is funded by the National Institute on Aging, the National Institute of Biomedical Imaging, and Bioengineering, and through contributions from the following: AbbVie, Alzheimer's Association; Alzheimer's Drug Discovery Foundation; Araclon Biotech; BioClinica, Inc.; Biogen; Bristol-Myers Squibb Company; CereSpir, Inc.; Cogstate; Eisai Inc.; Elan Pharmaceuticals, Inc.; Eli Lilly and Company; EuroImmun; F. Hoffmann-La Roche Ltd. and its affiliated company Genentech, Inc.; Fujirebio; GE Healthcare; IXICO Ltd.; Janssen Alzheimer Immunotherapy Research & Development, LLC.; Johnson & Johnson Pharmaceutical Research & Development LLC.; Lumosity; Lundbeck; Merck & Co., Inc.; Meso Scale Diagnostics, LLC.; NeuroRx Research; Neurotrack Technologies; Novartis Pharmaceuticals Corporation; Pfizer Inc.; Piramal Imaging; Servier; Takeda Pharmaceutical Company; and Transition Therapeutics. The Canadian Institutes of Health Research is providing funds to support ADNI clinical sites in Canada. Private sector contributions are facilitated by the Foundation for the National Institutes of Health (www.fnih.org). Open Access funding enabled and organized by Projekt DEAL.

Availability of data and materials

All neuroimaging and neuropsychology data that were used in this study are available online at the ADNI data repository (adni.loni.usc.edu).

Ethics approval and consent to participate

Ethical approval was obtained by the ADNI investigators, and all study participants provided written informed consent.

Consent for publication

Not applicable.

Competing interests

The authors declare that they have no competing interests.

Received: 15 April 2020 Accepted: 5 October 2020
Published online: 19 October 2020

References

1. Schwartz WJ, Smith CB, Davidsen L, Savaki H, Sokoloff L, Mata M, et al. Metabolic mapping of functional activity in the hypothalamo-neurohypophysial system of the rat. Science. 1979;205(4407):723.
2. Anchisi D, Borroni B, Franceschi M, Kerrouche N, Kalbe E, Beuthien-Beumann B, et al. Heterogeneity of brain glucose metabolism in mild cognitive impairment and clinical progression to Alzheimer disease. JAMA Neurol. 2005;62(11):1728–33.
3. Small GW, Mazziotta JC, Collins MT, Baxter LR, Phelps ME, Mandelkern MA, et al. Apolipoprotein E type 4 allele and cerebral glucose metabolism in relatives at risk for familial Alzheimer disease. JAMA. 1995;273(12):942–7.
4. Oh H, Habeck C, Madison C, Jagust W. Covarying alterations in Aβ deposition, glucose metabolism, and gray matter volume in cognitively normal elderly. Human brain mapping. 2014;35(1):https://doi.org/10.1002/hbm.22173.
5. Benzinger TLS, Blazey T, Jack CR, Koeppe RA, Su Y, Xiong C, et al. Regional variability of imaging biomarkers in autosomal dominant Alzheimer's disease. Proc Natl Acad Sci U S A. 2013;110(47):E4502–E9.
6. Yi D, Lee DY, Sohn BK, Choe YM, Seo EH, Byun MS, et al. Beta-amyloid associated differential effects of APOE ε4 on brain metabolism in cognitively normal elderly. Am J Geriatr Psychiatry. 2014;22(10):961–70.
7. Ashraf A, Fan Z, Brooks DJ, Edison P. Cortical hypermetabolism in MCI subjects: a compensatory mechanism? Eur J Nucl Med Mol Imaging. 2015;42(3):447–58.
8. Edison P, Archer HA, Hinz R, Hammers A, Pavese N, Tai YF, et al. Amyloid, hypometabolism, and cognition in Alzheimer disease: an [11C]PIB and [18F]FDG PET study. Neurology. 2007;68(7):501–8.
9. Ewers M, Insel P, Jagust WJ, Shaw L, Trojanowski JJ, Aisen P, et al. CSF biomarker and PIB-PET-derived beta-amyloid signature predicts metabolic, gray matter, and cognitive changes in nondemented subjects. Cereb Cortex. 2012;22(9):1993–2004.
10. Li Y, Rinne JO, Mosconi L, Pirraglia E, Rusinek H, DeSanti S, et al. Regional analysis of FDG and PIB-PET images in normal aging, mild cognitive impairment, and Alzheimer's disease. Eur J Nucl Med Mol Imaging. 2008;35(12):2169–81.
11. Rabinovici GD, Jagust WJ, Furst AJ, Ogar JM, Racine CA, Mormino EC, et al. Abeta amyloid and glucose metabolism in three variants of primary progressive aphasia. Ann Neurol. 2008;64(4):388–401.
12. Whitwell JL, Graff-Radford J, Tosakulwong N, Weigand SD, Machulda MM, Senjem ML, et al. Imaging correlations of tau, amyloid, metabolism, and atrophy in typical and atypical Alzheimer's disease. Alzheimers Dement. 2018;14(8):1005–14.
13. Ossenkoppele R, Schonhaut DR, Schöll M, Lockhart SN, Ayakta N, Baker SL, et al. Tau PET patterns mirror clinical and neuroanatomical variability in Alzheimer's disease. Brain. 2016;139(5):1551–67.
14. Dronse J, Fliessbach K, Bischof GN, von Reutern B, Faber J, Hammes J, et al. In vivo patterns of tau pathology, amyloid-beta burden, and neuronal dysfunction in clinical variants of Alzheimer's disease. J Alzheimers Dis. 2017;55(2):465–71.
15. Adams JN, Lockhart SN, Li L, Jagust WJ. Relationships between tau and glucose metabolism reflect Alzheimer's disease pathology in cognitively normal older adults. Cerebral Cortex. 2018:bhy078-bhy.
16. Hanseeuw BJ, Betensky RA, Schultz AP, Papp KV, Mormino EC, Sepulcre J, et al. Fluorodeoxyglucose metabolism associated with tau-amyloid interaction predicts memory decline. Ann Neurol. 2017;81(4):583–96.
17. Weigand AJ, Bangen KJ, Thomas KR, Delano-Wood L, Gilbert PE, Brickman AM, et al. Is tau in the absence of amyloid on the Alzheimer's continuum?: a study of discordant PET positivity. Brain Commun. 2020;2(1):fcz046.
18. Franzmeier N, Duering M, Weiner M, Dichgans M, Ewers M, For the Alzheimer's Disease Neuroimaging I. Left frontal cortex connectivity underlies cognitive reserve in prodromal Alzheimer disease. Neurology. 2017;88(11):1054–1061.
19. Petersen RC, Aisen PS, Beckett LA, Donohue MC, Gamst AC, Harvey DJ, et al. Alzheimer's Disease Neuroimaging Initiative (ADNI): clinical characterization. Neurology. 2010;74(3):201–9.
20. Hansson O, Seibyl J, Stomrud E, Zetterberg H, Trojanowski JQ, Bittner T, et al. CSF biomarkers of Alzheimer's disease concord with amyloid-β PET and predict clinical progression: a study of fully automated immunoassays in BioFINDER and ADNI cohorts. Alzheimer's & Dementia: The Journal of the Alzheimer's Association.
21. Jagust WJ, Landau SM, Koeppe RA, Reiman EM, Chen K, Mathis CA, et al. The ADNI PET core: 2015. Alzheimer's Dementia. 2015;11(7):757–71.
22. Lowe VJ, Curran G, Fang P, Liesinger AM, Josephs KA, Parisi JE, et al. An autoradiographic evaluation of AV-1451 Tau PET in dementia. Acta Neuropathologica Communications. 2016;4:58.
23. Landau SM, Mintun MA, Joshi AD, Koeppe RA, Petersen RC, Aisen PS, et al. Amyloid deposition, hypometabolism, and longitudinal cognitive decline. Ann Neurol. 2012;72(4):578–86.
24. Crane PK, Carle A, Gibbons LE, Insel P, Mackin RS, Gross A, et al. Development and assessment of a composite score for memory in the Alzheimer's Disease Neuroimaging Initiative (ADNI). Brain Imaging Behavior. 2012;6(4):502–16.
25. Mathotaarachchi S, Wang S, Shin M, Pascoal TA, Benedet AL, Kang MS, et al. VoxelStats: a MATLAB package for multi-modal voxel-wise brain image analysis. Front Neuroinformatics. 2016;10:20.
26. Worsley KJ, Marrett S, Neelin P, Vandal AC, Friston KJ, Evans AC. A unified statistical approach for determining significant signals in images of cerebral activation. Hum Brain Mapp. 1996;4(1):58–73.
27. Cook RD. Detection of influential observation in linear regression. Technometrics. 1977;19(1):15–8.
28. Merlo S, Spampinato SF, Sortino MA. Early compensatory responses against neuronal injury: a new therapeutic window of opportunity for Alzheimer's disease? CNS Neurosci Ther. 2019;25(1):5–13.
29. Cohen AD, Price JC, Weissfeld LA, James J, Rosario BL, Bi W, et al. Basal cerebral metabolism may modulate the cognitive effects of Aβ in mild cognitive impairment: an example of brain reserve. J Neurosci. 2009;29(47):14770–8.
30. Putcha D, Brickhouse M, O'Keefe K, Sullivan C, Rentz D, Marshall G, et al. Hippocampal hyperactivation associated with cortical thinning in Alzheimer's disease signature regions in non-demented elderly adults. J Neurosci. 2011;31(48):17680–8.
31. Clement F, Belleville S. Effect of disease severity on neural compensation of item and associative recognition in mild cognitive impairment. J Alzheimers Dis. 2012;29(1):109–23.
32. Quiroz YT, Budson AE, Celone K, Ruiz A, Newmark R, Castrillon G, et al. Hippocampal hyperactivation in presymptomatic familial Alzheimer's disease. Ann Neurol. 2010;68(6):865–75.
33. Dickerson BC, Salat DH, Greve DN, Chua EF, Rand-Giovannetti E, Rentz DM, et al. Increased hippocampal activation in mild cognitive impairment compared to normal aging and AD. Neurology. 2005;65(3):404–11.
34. Marks SM, Lockhart SN, Baker SL, Jagust WJ. Tau and beta-amyloid are associated with medial temporal lobe structure, function, and memory encoding in normal aging. J Neurosci. 2017;37(12):3192–201.
35. Huijbers W, Schultz AP, Papp KV, LaPoint MR, Hanseeuw B, Chhatwal JP, et al. Tau accumulation in clinically normal older adults is associated with hippocampal hyperactivity. J Neurosci. 2019;39(3):548–56.
36. Schultz AP, Chhatwal JP, Hedden T, Mormino EC, Hanseeuw BJ, Sepulcre J, et al. Phases of hyperconnectivity and hypoconnectivity in the default mode and salience networks track with amyloid and tau in clinically normal individuals. J Neurosci. 2017;37(16):4323–31.
37. Crary JF, Trojanowski JQ, Schneider JA, Abisambra JF, Abner EL, Alafuzoff I, et al. Primary age-related tauopathy (PART): a common pathology associated with human aging. Acta Neuropathol. 2014;128(6):755–66.
38. Bell WR, An Y, Kageyama Y, English C, Rudow GL, Pletnikova O, et al. Neuropathologic, genetic, and longitudinal cognitive profiles in primary age-related tauopathy (PART) and Alzheimer's disease. Alzheimers Dement. 2019;15(1):8–16.
39. Duyckaerts C, Braak H, Brion JP, Buee L, Del Tredici K, Goedert M, et al. PART is part of Alzheimer disease. Acta Neuropathol. 2015;129(5):749–56.
40. Bright J, Hussain S, Dang V, Wright S, Cooper B, Byun T, et al. Human secreted tau increases amyloid-beta production. Neurobiol Aging. 2015;36(2):693–709.
41. Roberson ED, Halabisky B, Yoo JW, Yao J, Chin J, Yan F, et al. Amyloid-β/Fyn–induced synaptic, network, and cognitive impairments depend on tau levels in multiple mouse models of Alzheimer's disease. J Neurosci. 2011;31(2):700.

42. Das M, Maeda S, Hu B, Yu GQ, Guo W, Lopez I, et al. Neuronal levels and sequence of tau modulate the power of brain rhythms. Neurobiol Dis. 2018; 117:181–8.
43. Levenga J, Krishnamurthy P, Rajamohamedsait H, Wong H, Franke TF, Cain P, et al. Tau pathology induces loss of GABAergic interneurons leading to altered synaptic plasticity and behavioral impairments. Acta Neuropathologica Communications. 2013;1(1):34.
44. Palop JJ, Chin J, Roberson ED, Wang J, Thwin MT, Bien-Ly N, et al. Aberrant excitatory neuronal activity and compensatory remodeling of inhibitory hippocampal circuits in mouse models of Alzheimer's disease. Neuron. 2007; 55(5):697–711.
45. Busche MA, Wegmann S, Dujardin S, Commins C, Schiantarelli J, Klickstein N, et al. Tau impairs neural circuits, dominating amyloid-β effects, in Alzheimer models in vivo. Nat Neurosci. 2019;22(1):57–64.
46. Pooler AM, Phillips EC, Lau DHW, Noble W, Hanger DP. Physiological release of endogenous tau is stimulated by neuronal activity. EMBO Rep. 2013;14(4): 389–94.
47. Wu JW, Hussaini SA, Bastille IM, Rodriguez GA, Mrejeru A, Rilett K, et al. Neuronal activity enhances tau propagation and tau pathology in vivo. Nat Neurosci. 2016;19(8):1085–92.
48. Apostolova I, Lange C, Maurer A, Suppa P, Spies L, Grothe MJ, et al. Hypermetabolism in the hippocampal formation of cognitively impaired patients indicates detrimental maladaptation. Neurobiol Aging. 2018;65:41–50.
49. Bakker A, Krauss Gregory L, Albert Marilyn S, Speck Caroline L, Jones Lauren R, Stark Craig E, et al. Reduction of hippocampal hyperactivity improves cognition in amnestic mild cognitive impairment. Neuron. 2012;74(3):467–74.
50. Heneka MT, Carson MJ, El Khoury J, Landreth GE, Brosseron F, Feinstein DL, et al. Neuroinflammation in Alzheimer's disease. Lancet Neurol. 2015;14(4): 388–405.
51. Abner EL, Kryscio RJ, Schmitt FA, Fardo DW, Moga DC, Ighodaro ET, et al. Outcomes after diagnosis of mild cognitive impairment in a large autopsy series. Ann Neurol. 2017;81(4):549–59.
52. Schneider JA, Arvanitakis Z, Leurgans SE, Bennett DA. The neuropathology of probable Alzheimer disease and mild cognitive impairment. Ann Neurol. 2009;66(2):200–8.
53. Rahimi J, Kovacs GG. Prevalence of mixed pathologies in the aging brain. Alzheimers Res Ther. 2014;6(9):82.
54. Nelson PT, Trojanowski JQ, Abner EL, Al-Janabi OM, Jicha GA, Schmitt FA, et al. "New old pathologies": AD, PART, and cerebral age-related TDP-43 with sclerosis (CARTS). J Neuropathol Exp Neurol. 2016;75(6):482–98.
55. Brendel M, Focke C, Blume T, Peters F, Deussing M, Probst F, et al. Time courses of cortical glucose metabolism and microglial activity across the life span of wild-type mice: a PET study. J Nuclear Med. 2017;58(12):1984–90.
56. Herholz K, Boecker H, Nemeth I, Dunn G. FDG PET in dementia multicenter studies and clinical trials. Clin Translational Imaging. 2013;1(4):261–70.

Publisher's Note

Supplementary

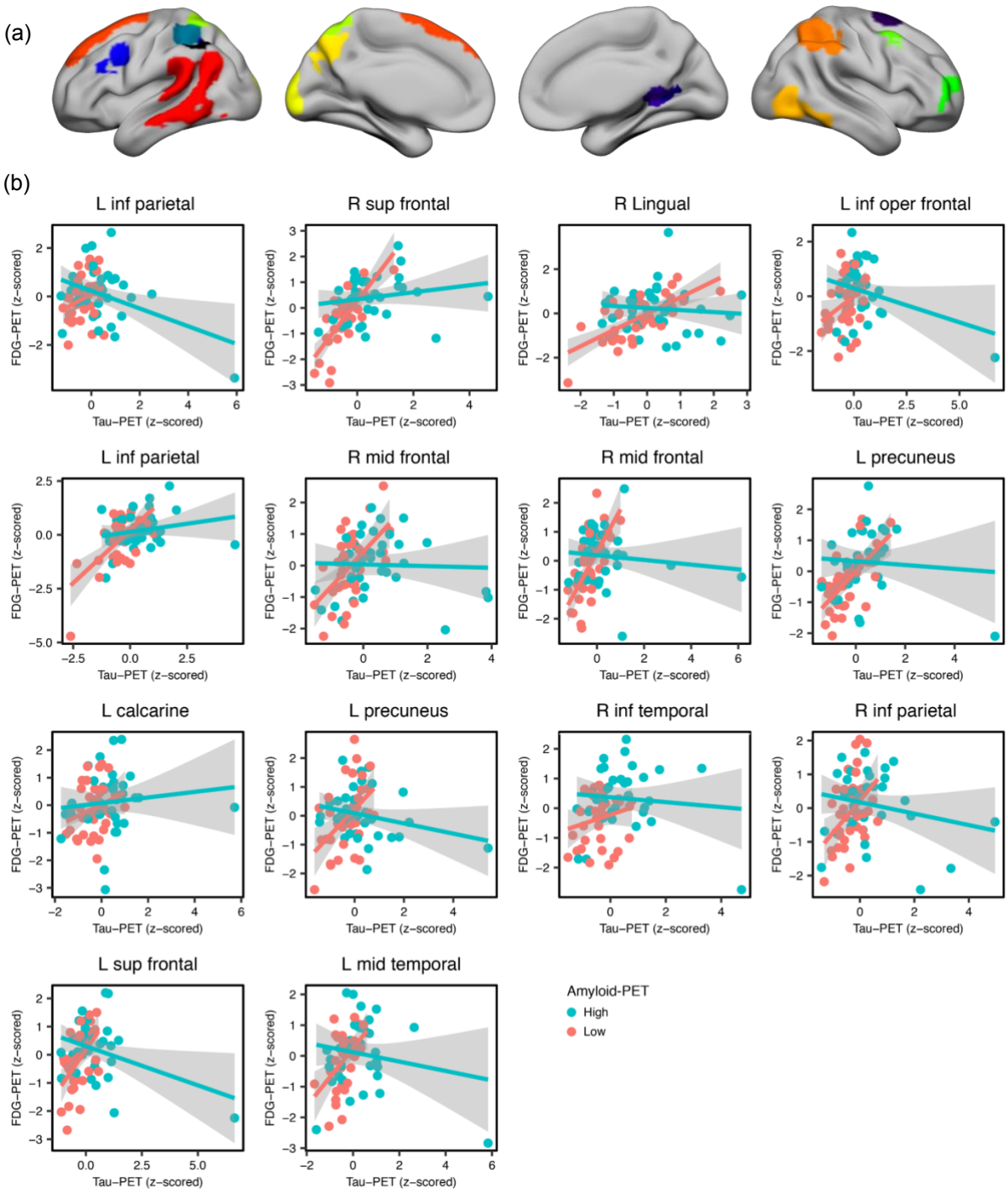

Supplementary Figure 1: Regional interactions between amyloid- and tau-PET on FDG-PET metabolism in MCI. (a) Projection of significant clusters resulting from the voxel-wise analysis. (b) Scatterplots are based on mean SUVR values extracted from voxel-wise analyses for each of the significant clusters (arranged by anatomical adjacency). Amyloid was used as a continues measure, for illustrational purposes amyloid levels were stratified to high and low (median split).

Supplementary Table 1: Areas showing significant voxel-wise effect of amyloid-PET and tau-PET on FDG-PET in MCI.

Size (voxels)	T-value	MNI coordinates		
		x	Y	z
Main effect of amyloid-PET on FDG-PET				
Positive association				
590	4.94	24	15	-31.5
472	3.76	24	-90	30
335	3.82	-18	12	69
220	4.25	-4.5	-85.5	39
180	4.35	-13.5	-12	76.5
Main effect of tau-PET on FDG-PET				
Positive association				
10844	7.55	4.5	-43.5	67.5
4312	6.66	-4.5	-45	70.5
1439	5.05	-64.5	-12	27
748	5.7	-49.5	-24	10.5
410	4.28	-34.5	-21	3
397	4.84	15	70.5	9
328	5.1	-4.5	-93	-18
244	5.81	28.5	-55.5	9
212	4.91	-24	-54	6
183	4.77	-1.5	45	15
Negative association				
2124	4.94	-28.5	45	16.5
1251	4.94	-49.5	-52.5	9
564	4.62	24	-76.5	-10.5
Main effect of tau-PET on FDG-PET in Aβ+ subjects				
Positive association				
935	5.49	-46.5	-30	9
280	4.67	42	-15	15
241	5.34	4.5	-42	64.5
Negative association				
5725	7.07	-57	-48	-10.5
2723	7.12	-34.5	6	51
1878	6.61	30	-90	3
587	5.25	-10.5	-57	46.5
421	5.57	-48	25.5	7.5
322	5.2	45	-52.5	42
Main effect of tau-PET on FDG-PET in Aβ- subjects				
Positive association				
4262	5.85	36	-21	63
3091	6.96	-21	-22.5	75
533	4.85	27	57	13.5
504	4.39	55.5	-37.5	54
433	4.54	3	46.5	3
406	5.76	52.5	19.5	30
285	4.92	-19.5	-48	72
243	4.44	-57	-63	-16.5
220	4.67	-45	6	16.5
220	4.06	21	54	28.5

MNI coordinates and t-values of the peaks are provided. T-values are based on voxel-wise regressions controlling for age, gender, education, study site and amyloid/tau-PET. (*L, Left; R, Right).*

Manuscript 2

Rubinski, A., Tosun, D., Franzmeier, N., Neitzel, J., Frontzkowski, L., Weiner, M., & Ewers, M. (2021). Lower cerebral perfusion is associated with tau-PET in the entorhinal cortex across the Alzheimer's continuum. *Neurobiology of Aging, 102*, 111-118.

DOI: 10.1016/j.neurobiolaging.2021.02.003

Contributions: AR is the first author on this manuscript, AR designed the study, conducted the analyses, interpreted the results, and drafted the manuscript, DT analyzed the data and provided critical review of the manuscript, NF and JN provided critical review of the manuscript, LF processed the data, MW provided critical review of the manuscript, ME designed the study, interpreted the results, and drafted the manuscript.

Neurobiology of Aging 102 (2021) 111–118

Contents lists available at ScienceDirect

Neurobiology of Aging

journal homepage: www.elsevier.com/locate/neuaging.org

Lower cerebral perfusion is associated with tau-PET in the entorhinal cortex across the Alzheimer's continuum

Anna Rubinski[a], Duygu Tosun[b], Nicolai Franzmeier[a], Julia Neitzel[a], Lukas Frontzkowski[a], Michael Weiner[b], Michael Ewers[a,c,*]

[a] Institute for Stroke and Dementia Research, Klinikum der Universität München, Ludwig-Maximilians-Universität LMU, Munich, Germany
[b] Department of Radiology and Biomedical Imaging, University of California, San Francisco, USA
[c] German Center for Neurodegenerative Diseases, Munich, Germany

ARTICLE INFO

Article history:
Received 22 September 2020
Revised 1 February 2021
Accepted 4 February 2021
Available online 10 February 2021

Keywords:
Alzheimer's Disease (AD)
Tau-PET
Amyloid-PET
Arterial Spin Labeling (ASL)
Cerebral Blood Flow (CBF)

ABSTRACT

Alzheimer's disease (AD) is associated with reduced temporo-parietal cerebral blood flow (CBF). However, a substantial variability in CBF across the clinical spectrum of AD has been reported, possibly due to differences in primary AD pathologies. Here, we assessed CBF (ASL-MRI), tau (AV1451-PET) and amyloid (AV45/FBB-PET) in 156 subjects across the AD continuum. Using mixed-effect regression analyses, we assessed the local associations between amyloid-PET, tau-PET and CBF in a hypothesis-driven way focusing on each pathology's predilection areas. The contribution of Apolipoprotein E (APOE) genotype, and MRI markers of small vessel disease (SVD) to alterations in CBF were assessed as well. Tau-PET was associated with lower CBF in the entorhinal cortex, independent of Aβ. Amyloid-PET was associated with lower CBF in temporo-parietal regions. No associations between MRI markers of SVD and CBF were observed. These results provide evidence that in addition to Aβ, pathologic tau is a major correlate of CBF in early Braak stages, independent of Aβ, APOE genotype and SVD markers.

1. Introduction

Reduced perfusion of the brain tissue is a common pathological alteration in Alzheimer's disease (AD) (Love and Miners, 2016). Alterations in perfusion, including lower cerebral blood flow (CBF), are predictive of cognitive decline (Xekardaki et al., 2015) and the conversion from mild cognitive impairment (MCI) to AD (Chao et al., 2010), rendering CBF measurement as a candidate biomarker of dementia risk (Wolters et al., 2017). CBF can be quantified using an arterial spin labeling (ASL) MRI sequence which uses magnetically labeled endogenous arterial blood water as a tracer (Wolf and Detre, 2007). Therefore, it provides a radiation free and noninvasive measure of CBF, and thus a clinically attractive alternative over radioactive tracers (Chen et al., 2011; Tosun et al., 2016).

Despite CBF alterations being common in AD, their link to primary pathologies including Aβ and fibrillar tau remains unclear. Previously, a correlation between higher amyloid-PET and lower CBF was demonstrated across the spectrum of sporadic AD (Mattsson et al., 2014; Tosun et al., 2014) and autosomal dominant AD (McDade et al., 2014). However, no significant CBF reductions were observed in nondemented elderly who had abnormal CSF A$\beta_{1\text{-}42}$ yet normal CSF t-tau (Binnewijzend et al., 2016). Accumulating evidence shows that CSF tau proteins are associated with lower CBF in cognitively normal (CN) individuals (Stomrud et al., 2012) as well as in patients with MCI and AD dementia (Habert et al., 2010). These in vivo findings are corroborated by brain autopsy studies reporting that antemortem CBF reduction in AD is related to higher postmortem Braak stages of tau pathology (Bradley et al., 2002). However, neither postmortem histochemical analyses nor CSF biomarker studies allow for assessing region-specific effects of tau pathology on CBF. Moreover, given that Aβ deposition is a strong predictor of tau accumulation (Jack et al., 2018), any association between tau and CBF may be related to Aβ deposition. Therefore, the main focus of the current study was to test whether local tau-PET is associated with lower CBF in spatially corresponding brain regions, with and without controlling for the contribution of Aβ.

Here, we examined the regional associations between CBF (pseudo-continues ASL; pCASL), fibrillar tau ([^{18}F]AV1451-PET) and Aβ ([^{18}F]AV45/([^{18}F]FBB-PET) in spatially matched regions of inter-

* Corresponding author at: Institute for Stroke and Dementia Research (ISD), Klinikum der Universität München, Feodor-Lynen-Straße 17, D-81377 Munich, Germany, Tel: +49 (0)89 4400 - 461221; fax: +49 (0)89 4400 – 46000.
E-mail address: Michael.Ewers@med.uni-muenchen.de (M. Ewers).

0197-4580/$ – see front matter © 2021 Elsevier Inc. All rights reserved.
https://doi.org/10.1016/j.neurobiolaging.2021.02.003

est (ROIs). We restricted these ROI analyses in a hypothesis-driven manner to each pathology's predilection areas, that is, Braak-stage ROIs for tau-PET, and the default-mode-network (DMN) ROIs for amyloid-PET.

Furthermore, small vessel disease (SVD) is common both in aging and AD. Previous studies have shown that MRI proxies of SVD, namely, higher number of microbleeds (Gregg et al., 2015) and higher white matter hyperintensity (WMH) volume (Shi et al., 2016; Kim et al., 2020) are associated with reduced CBF. Since increased tau-PET levels are also observed in subjects with SVD (Kim et al., 2018), it is possible that any associations between tau and CBF are mediated by SVD.

Therefore, we assessed the contribution of markers of SVD including WMH and cerebral microbleeds in addition to tau-PET and amyloid-PET as predictors of CBF.

2. Methods

2.1. Participants

We included a sample of 156 participants comprised of CN (n = 84), amnestic MCI (n = 51) and AD dementia (n = 21) which were assessed at a total of 14 study sites within the Alzheimer's Disease Neuroimaging Initiative (ADNI; recruitment phase III). Beyond the inclusion criteria of ADNI, additional requirements comprised availability of 3D pCASL images and [^{18}F]AV1451 tau-PET obtained no longer than 12 months apart (mean 30.72 ± 39.78 days apart). In addition, 145 participants had either [^{18}F]AV45 amyloid-PET (n = 82) or [^{18}F]FBB amyloid-PET (n = 63) scans acquired within 12 months from the pCASL scan (mean 76.41 ± 115.32 days apart). Apolipoprotein E (APOE) genotyping was available in a subset of 140 participants.

The diagnostic criteria of CN in ADNI included a Mini Mental State Exanimation (MMSE) score ≥ 24, Clinical Dementia Rating (CDR) = 0 and no memory concerns (Petersen et al., 2010). Amnestic MCI participants had MMSE score ≥ 24, CDR = 0.5, subjective memory concern, objective memory loss measured by education adjusted scores on the Wechsler Memory Scale Memory II, absence of significant levels of impairment in other cognitive domains, essentially preserved activities of daily living and an absence of dementia (Petersen et al., 2010). AD dementia participants had MMSE score ≤ 26, CDR > 0.5 and fulfillment of NINCDS/ADRDA criteria for probable Alzheimer's disease (Petersen et al., 2010).

Ethical approval was obtained by the ADNI investigators, all participants provided written informed consent (further information about the inclusion/exclusion criteria may be found at www.adni-info.org).

2.2. T1 acquisition and preprocessing

All imaging data were downloaded from the ADNI LONI image archive (https://ida.loni.usc.edu). All MRI data were obtained on 3T General Electric (GE) MRI scanner according to standardized protocol within ADNI phase III. 3D T1-weighted scans were acquired using an accelerated Fast Spoiled Gradient Echo with Inversion Recovery-Preparation (IR-FSPGR) sequence, 1 mm isotropic resolution and a TR/TE/Flip angle = 7.3–7.7 s/3.05–3.12 ms/11°.

For each participant, we applied volumetric segmentation to the native-space structural images using FreeSurfer-based pipeline (version 6.0; freesurfer.net), in which subcortical and cortical areas are segmented automatically using the probabilistic Desikan-Killiany atlas (Desikan et al., 2006).

2.3. ASL acquisition and preprocessing

ASL-MRI scans were acquired using a 3D pCASL sequence on exclusively GE scanners with resolution = 1.9 × 1.9 × 4 mm^3 and a TR/TE/Flip angle = 4.9 s/10.5–10.7 ms/111°. ASL images were preprocessed with ExploreASL, an automated MATLAB based toolbox for ASL analysis (Mutsaerts et al., 2020). Quantitative CBF images were estimated based on recommended modeling for clinical applications (Alsop et al., 2015). The major assumptions of this model included homogeneous blood/brain partition coefficient of 0.9 mL/g for water, labeling inversion efficiency of 80%, background suppression efficiency of 75% and T1 of blood at 1.6 s. The partial saturation of the reference proton density image was corrected for by using a T1t of 1.2 s, typical of GM. The difference between the corrected proton density image and the perfusion weighted image, yielding the quantitative CBF in mL/100 g/min units of arterial water density. Partial volume effect (PVE) correction was performed using a spatial linear regression algorithm to estimate the flow contribution of each tissue at a given voxel as described previously (Asllani et al., 2008; Petr et al., 2018). All statistical analyses were computed based on PVE corrected CBF data.

PVE corrected CBF images in the participant's T1 space were resliced using SPM12 (Wellcome Trust Centre for Neuroimaging, University College London) to T1 resolution and ROI based values were extracted based on FreeSurfer anatomical parcellations from the T1 images. Regional CBF values were residualized by the mean signal of the precentral gyrus as the reference region in order to render comparability to earlier studies on the associations between amyloid-PET and ASL assessed CBF (Mattsson et al., 2014; Yew et al., 2017).

2.4. [18F]AV1451 tau-PET and [^{18}F]AV45/[^{18}F]FBB amyloid-PET acquisition and preprocessing

Tau-PET data were acquired for 30 minutes dynamic emission scan, six 5-minutes frames, 75105 minutes postinjection of 10.0 mCi of [^{18}F]AV1451. Amyloid-PET data were acquired for 20 minutes dynamic emission scan, four 5-minutes frames, 50–70 minutes post injection of 10.0 mCi of [^{18}F]AV45 or 20 minutes dynamic scan, four 5-minutes frames, 90–110 minutes post injection of 8.1 mCi of [^{18}F]FBB.

Final datasets including amyloid-PET and tau-PET ROI values were downloaded from the ADNI website. PET quality control and preprocessing were centrally conducted at the ADNI PET core center at University of California Berkeley as previously described (Jagust et al., 2015). The preprocessing steps included frame coregistration, averaging across the dynamic range and standardization with respect to the orientation, voxel size and intensity and smoothing to produce images of a uniform isotropic resolution of 8 mm FWHM (Jagust et al., 2015). Tau-PET scans were corrected for partial volume effects using the Geometric Transfer Matrix approach as previously described (Baker et al., 2017). Preprocessed PET images were subsequently coregistered to the participant's T1 image in native-space and FreeSurfer-based anatomical parcellations were applied to extract ROI based values. Standardized uptake value ratio (SUVR) scores were obtained by normalizing ROI values to the mean uptake of the whole cerebellum for amyloid-PET data, and to the mean uptake of the inferior cerebellar GM for tau-PET data, following previous recommendations (Landau et al., 2012; Maass et al., 2017).

2.5. Assessment of amyloid status

82 participant underwent [^{18}F]AV45 amyloid-PET and 63 participants [^{18}F]FBB amyloid PET. Amyloid status was computed fol-

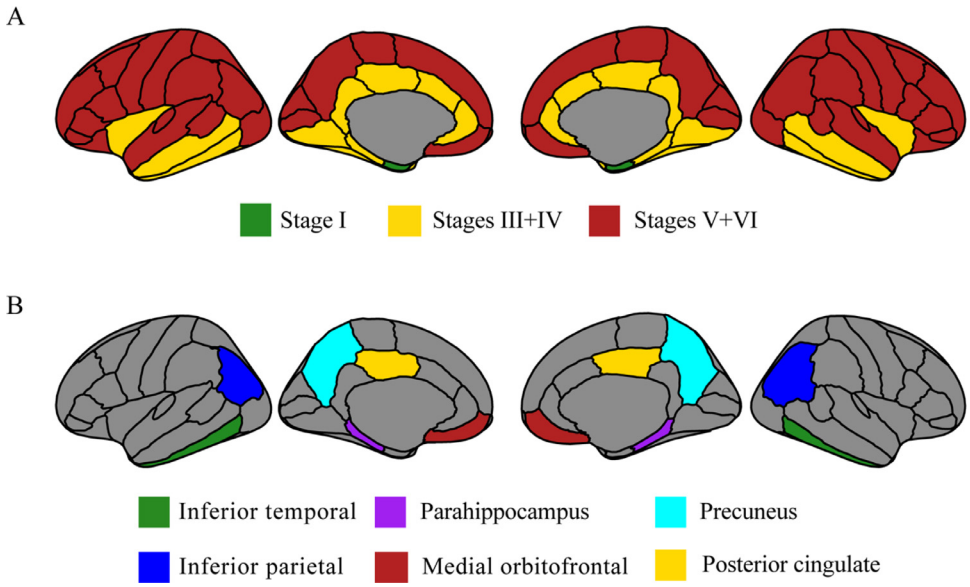

Fig. 1. (A) Spatial mapping of Braak stage-specific ROIs that were used to determine regional CBF and tau-PET uptake. For Braak stage II, the hippocampus was not included due to known off-target binding of the AV1451-PET tracer in that region. (B) Spatial mapping of default mode network ROIs that were used to determine regional CBF and amyloid-PET uptake.

lowing a method described previously (Landau et al., 2012). Briefly, the global cortical amyloid scores were calculated as a mean across FreeSurfer-derived cortical GM ROIs (frontal, lateral temporal, lateral parietal and anterior/posterior cingulate) divided by whole cerebellum reference region. Participants were classified as Aβ+ or Aβ- based on established cutoff values (global AV45-PET SUVR > 1.11 or global FBB-PET SUVR > 1.08) (Landau et al., 2012). To obtain comparable quantification of the amyloid burden across tracers, we used the following centiloid calculation as recommended for the ADNI pipeline: AV45 centiloid = 196.9 X $SUVR_{FBP}$ - 196.03, where $SUVR_{FBP}$ is the SUVR of AV45, and FBB centiloid = 159.08 X $SUVR_{FBB}$ − 151.65, where $SUVR_{FBB}$ is the SUVR of FBB).

2.6. A priori selection of ROIs

In order to test the association between tau-PET and CBF, we included ROIs defined by the Braak-staging (Fig. 1A). That is, average values for three composite ROIs scores including Braak stage I (entorhinal), Braak III/IV (limbic) and Braak V/VI (neocortical) were obtained for each modality including tau-PET, amyloid-PET and CBF. Braak stage II (hippocampus) was not included due to spill of from known off-target binding of the tau-PET tracer to choroid plexus (Marquie et al., 2015).

In order to test the association between amyloid-PET and CBF, we focused on DMN regions which are predilection areas of amyloid deposition early in the course of AD (Palmqvist et al., 2017). Values of amyloid-PET, tau-PET and CBF were extracted for 6 a priori designated ROIs within the DMN: medial-orbitofrontal, precuneus, posterior cingulate, inferior parietal, inferior temporal and parahippocampal gyrus (Fig. 1B). To obtain comparable quantification of the amyloid burden across tracers, we used the centiloid calculation mentioned above for regional amyloid-PET measures.

2.7. White matter hyperintensity segmentation

WMH volumes were extracted using T1 and Fluid-Attenuated Inversion Recovery (FLAIR) scans. 3D FLAIR scans were acquired with resolution = 1 × 1 × 1.2 mm^3 and a TR/TE/Flip angle = 4.8 s/119 ms/90°. Detailed information describing the assessment process is available online on the ADNI website (http://adni.loni.usc.edu/methods). The total WMH volume was divided by the total intracranial volume to obtain a normalized global WMH volume. Since WMHs typically have a skewed distribution, we applied an inverse-hyperbolic sine (IHS) transform to the WMH volume ratio, as reported previously (Caballero et al., 2020).

2.8. Cerebral microbleeds assessment

Cerebral microbleeds were defined as areas of signal void on T2*-weighted MRI and performed by ADNI MRI-Core (available for a subset of 155 participants). T2*-weighted scans were acquired with resolution = 0.85 × 0.85 × 4 mm^3 and a TR/TE/Flip angle = 650ms/20ms/20°. Relevant findings were cataloged with information about each observation of the finding on the associated T2* image. Findings cataloged as definite microbleeds were counted and used for further analysis. Detailed information describing the assessment process is available online on the ADNI website (http://adni.loni.usc.edu/methods).

2.9. Statistical analysis

Group demographics were compared between groups using Kruskal-Wallis for continuous measures (followed by Bonferroni-corrected post-hoc Dunn tests) and Chi-squared tests for categorical measures.

For all subsequent analysis on CBF, PVE-corrected values were used and for the sake of simplicity, we simply refer to CBF values. For our main analyses, we tested whether increased tau-PET was associated with reduced perfusion in Braak stage ROIs. To this end, we conducted mixed-effect regression analysis to test whether regional tau-PET levels are a significant predictor of participants' CBF in the 3 spatially matched composite Braak-stage ROIs, accounting for age, gender, diagnosis, education (fixed effects) and the study site as a random effect. Analyses were performed in the entire sample as well as in the nondemented subgroup (excluding AD dementia participants) or in subgroups defined by Aβ status. Division

Table 1
Sample characteristics, mean (SD)

Group	CN (n = 84)	MCI (n = 51)	AD (n = 21)	*p*-value
Age (years)	72.70 (6.49)	74.90 (8.05)	76.10 (6.16)	0.032
Gender (M / F)	36/48	31/20	14/7	0.045
Education (years)	16.71 (2.43)	16.65 (2.59)	15.76 (2.39)	0.199
MMSE	29.35 (0.88)	27.94 (2.41)*	22.38 (3.81)*,†	<0.001
Aβ-/Aβ+[a]	55-/25+	32-/15+	18+*,†	<0.001
APOE ε4 carriers -/+ [b]	52-/30+	27-/15+	4-/12+*,†	0.012
Global Aβ centiloid [a]	2.43 (28.65)	28.34 (45.88)	86.18 (31.39) *,†	<0.001
Global tau-PET SUVR	1.42 (0.15)	1.52 (0.33)	1.95 (0.95) *,†	<0.001
Global GM CBF [c] (mL/100g/min)	42.39 (9.73)	38.25 (10.38)	33.70 (12.31)*	<0.001
WMH volume (mL) [d]	3.13 (4.90)	4.28 (4.73)	6.22 (8.33)*	0.003
Microbleeds count [e]	0.45 (0.89)	0.75 (2.29)	0.57 (0.81)	0.604

Key: Aβ, amyloid-beta; AD, Alzheimer's disease; APOE, Apolipoprotein E; CBF, cerebral blood flow; CN, cognitively normal; F, female; GM, grey matter; M, male; MCI, mild cognitive impairment; MMSE, Mini-Mental State Exam; WMH, white matter hyperintensity.
* Significantly different from CN.
† Significantly different from MCI. (Significant after applying a Bonferroni-corrected α-threshold of 0.017).
[a] Available for 145 subjects.
[b] Available for 140 subjects.
[c] Data is PVE corrected.
[d] Raw, nontransformed data
[e] Available for 155 subjects.

to subgroups was performed in order to ensure that our results are not driven by extreme AD dementia cases or by Aβ burden.

Moreover, we checked whether there were few highly influential cases based on by Cook's distance D (Cook and Weisberg, 1982). Influential cases were defined as observations with Cook's distance exceeding the predefined threshold (calculated as 4/N; N=number of observations (Bollen and Jackman, 1985)). In case observations exceeding the threshold were detected, analyses were rerun excluding those observations to test for the robustness of the results.

To account for the effect of amyloid pathology, the main analyses were repeated with regional amyloid-PET centiloid or tau-PET x amyloid-PET centiloid as additional predictors. All models were controlled for age, gender, diagnosis, education (fixed effects) and the study site as a random effect.

Next, we tested whether increased global or regional amyloid-PET was associated with reduced perfusion in DMN ROIs, i.e. predilection areas of amyloid deposition. To this end, we conducted mixed-effect regression analyses with global or regional amyloid-PET centiloid in DMN ROIs, as predictors of CBF in spatially corresponding ROIs. The analyses were repeated with regional tau-PET as additional predictor. All models were controlled for age, gender, diagnosis, education (fixed effects) and the study site as a random effect.

Lastly, we tested the associations between MRI markers of SVD (WMH volume and microbleeds) and global CBF. To that end, we used linear mixed-effect regression model with IHS-transformed WMH ratio or the microbleeds count as the independent variable and global mean CBF as the dependent variable, accounting for age, gender, diagnosis, education (fixed effects) and study site (random effect).

All analyses were performed using R statistical software package (http://www.R-project.org). Associations (standardized beta coefficients and correlation) were considered significant when meeting an α-threshold of 0.05. Correction for multiple comparisons was done using Bonferroni correction.

2.10. Data availability statement

Data on participant demographics are available in Table 1. ADNI data are accessible from http://adni.loni.usc.edu/data-samples/access-data/.

Table 2
Linear mixed models testing the regional effects of tau-PET on CBF in the whole group (n = 156)

ROI	Tau	
	b/SE	*p*-value
Braak I	-0.371/0.088	<0.001*
Braak III/IV	-0.120/0.089	0.180
Braak V/VI	0.156/0.082	0.057

Models are controlled for age, gender, education, diagnosis (fixed effects) and study site (random effect).
* Remains significant after applying a Bonferroni-corrected α-threshold of 0.017 (i.e., $\alpha = 0.05$ adjusted for 3 tests).

3. Results

3.1. Sample characteristics

For the current study, we analyzed data from 156 participants of the ADNI cohort, including 84 CN, 51 MCI and 21 AD dementia subjects (see Table 1 for sample characteristics). After correction for multiple comparisons, there were no differences in baseline demographics (age, gender, education) as well as in microbleeds count between the different diagnostic groups. As expected, AD dementia subjects had lower MMSE score, higher frequency of Aβ positivity and APOE ε4 carriage, higher global Aβ centiloid, higher global tau-PET SUVR, lower mean global CBF, and higher WMH volume.

Regional distributions of amyloid-PET centiloid, tau-PET SUVRs and CBF within the sample are shown for the Desikan-Kiliany ROIs in supplementary Figure 1.

3.2. Higher tau-PET is associated with lower perfusion exclusively in the entorhinal cortex

In a first step, we tested the hypothesis that tau pathology is associated with reduced perfusion in Braak stage ROIs (Figure 1A). As shown in Fig. 2 (Table 2), we found that higher tau-PET was associated with lower CBF in the entorhinal cortex (Braak I: $\beta = -0.371$, SE = 0.088, $p < 0.001$) accounting for confounding effects of age, gender, diagnosis, education (fixed effects) and study site (random effect). After exclusion of nine outliers detected based on Cook's distance, the association between tau-PET and CBF in the entorhi-

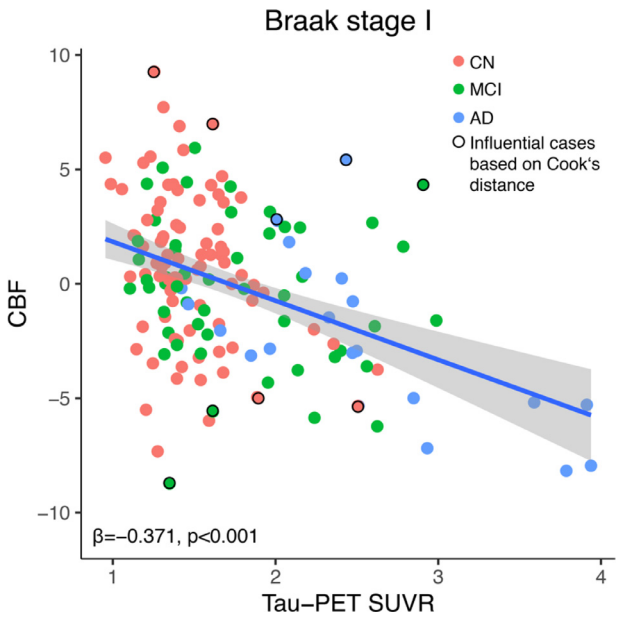

Fig. 2. Higher tau-PET is associated with lower CBF in the entorhinal cortex (Braak stage I).

nal cortex remained significant (Braak I: β = -0.423, SE = 0.088, p < 0.001). There were no significant associations between tau-PET and CBF in Braak stage ROIs III/IV and V/VI (p = 0.180 and p = 0.057 respectively). The association in the entorhinal cortex remained significant after applying a Bonferroni-corrected α-threshold of 0.017 (i.e., α = 0.05 adjusted for 3 tests).

To test whether the association between tau-PET and CBF in the entorhinal cortex is independent of Aβ, as a first step we split the sample into Aβ- and Aβ+ subgroups. We found significant associations both in the Aβ+ subgroup (Braak I: β = -0.485, SE = 0.139, p = 0.001), and the Aβ- subgroup (Braak I: β = -0.313, SE = 0.095, p = 0.002). Similarly, inclusion of regional amyloid-PET as a covariate in the main analysis did not alter the association between tau-PET and CBF in the entorhinal cortex (Braak I: β = -0.363, SE = 0.095, p < 0.001). No interaction between regional tau-PET and regional amyloid-PET centiloid was observed.

To ensure that our results are not driven by extreme AD dementia cases, we repeated the analysis in a nondemented subgroup (consists of 84 CN and 51 MCI participants). We found that the association between higher tau-PET and lower CBF remained significant in the entorhinal cortex (Braak I: β = -0.236, SE = 0.086, p = 0.007).

As exploratory analysis we also tested the effect of APOE genotype on the association between tau-PET and CBF. Inclusion of APOE status as a covariate in the main analysis did not alter the association between tau-PET and CBF in the entorhinal cortex (Braak I: β = -0.412, SE = 0.095, p < 0.001). We found a significant association of tau-PET and CBF, both in the APOE e4- non-carriers subgroups (Braak I: β = -0.397, SE = 0.111, p < 0.001) as well as in the APOE e4+ carriers subgroup (Braak I: β = -0.372, SE = 0.162, p = 0.026). No interaction between regional tau-PET and APOE genotype was observed. See supplementary Table 1 for detailed statistics.

3.3. Higher global and regional amyloid-PET are associated with reduced perfusion in temporo-parietal regions

We tested whether CBF is associated with global or regional amyloid-PET centiloid in DMN ROIs (Fig. 1B). As shown in Fig. 3 (Table 3), higher global amyloid-PET centiloid was associated with lower CBF in the inferior temporal (β = -0.367, SE = 0.083, p < 0.001), inferior parietal (β = -0.259, SE = 0.076, p < 0.001), and precuneus (β = -0.214, SE = 0.085, p = 0.013). Associations in the inferior temporal and the inferior parietal remained significant after applying a Bonferroni-corrected α-threshold of 0.008 (i.e., α = 0.05 adjusted for 6 tests). Similar results were observed when testing the associations between regional amyloid-PET centiloid and CBF.

Table 3
Linear mixed models testing the effects of global amyloid-PET on CBF in the amyloid subsample (n = 145)

ROI	Aβ	
	b/SE	p-value
Inferior temporal	-0.367/0.083	<0.001*
Parahippocampus	-0.094/0.092	0.305
Inferior parietal	-0.259/0.076	<0.001*
Posterior cingulate	0.041/0.087	0.637
Precuneus	-0.214/0.085	0.013
Medial orbitofrontal	-0.042/0.082	0.610

Models are controlled for age, gender, education, diagnosis (fixed effects) and study site (random effect).
* Remains significant after applying a Bonferroni-corrected α-threshold of 0.008 (i.e., α = 0.05 adjusted for 6 tests).

When including in the model tau-PET obtained in the same ROIs, the association between global amyloid-PET centiloid and CBF remained unchanged in the inferior temporal and the precuneus. However, in the inferior parietal, global amyloid-PET centiloid no longer had a significant association with CBF, instead, an association between tau-PET and CBF (β = -0.336, SE = 0.083, p < 0.001) was observed. See supplementary Table 2 for detailed statistics.

3.4. CBF is not associated with MRI markers of SVD

In order to ensure that our results are not driven by vascular factors, we tested the association between MRI markers of SVD (WMH volume and microbleeds) and CBF. No associations between global mean CBF and WMH volume (p = 0.77) or microbleeds count (p = 0.56) were observed.

4. Discussion

Our main findings show an association between higher tau-PET and lower CBF in the entorhinal cortex, independent of Aβ pathology. For Aβ, higher global and regional amyloid-PET were associated with reduced CBF in temporo-parietal regions, even after controlling for tau-PET in the same ROIs. There were no associations between MRI-markers of SVD and CBF. Together, these results suggest that pathologic tau, is a major correlate of lower CBF in early Braak stages, independent of Aβ, SVD markers and APOE genotype.

Our dual-tracer assessment of Aβ and tau pathology allowed to discern the roles of each pathology in local decreases in CBF. Our results provide an important advance beyond previous reports that focused only on the association between amyloid-PET and CBF (Bangen et al., 2017; Hansson et al., 2018; Mattsson et al., 2014; McDade et al., 2014; Michels et al., 2016; Rodell et al., 2016). Our results of the association between tau-PET and lower perfusion are in general agreement with previous findings on the association between higher levels of CSF biomarkers of tau and perfusion in cognitively normal APOE e4 carriers (Hays et al., 2020) and postmortem findings of higher Braak-stages of tau pathology to be associated with higher expression of the vascular endothelial

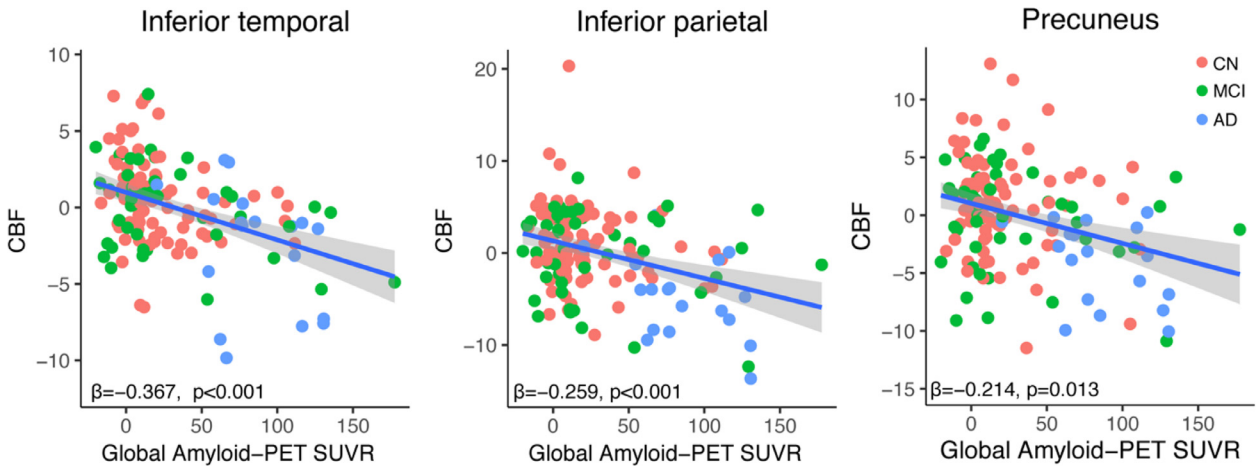

Fig. 3. Higher global amyloid-PET is associated with lower CBF in the inferior temporal, inferior parietal and precuneus.

growth factor (VEGF), i.e. a marker of hypoperfusion related hypoxia (Thomas et al., 2015). Interestingly, tau-PET was associated also with lower CBF in the inferior parietal in the secondary analysis focusing on predilection areas of Aβ, suggesting that also subtle elevations of tau-PET are related to lower perfusion. Together these findings suggest that local associations of tau-PET and CBF are strongest in the entorhinal cortex, but tau pathology may drive amyloid related changes in CBF also in other higher cortical areas.

We found associations between global as well as regional amyloid-PET and lower temporo-parietal perfusion. While our findings are in agreement with previous reports (Mattsson et al., 2014; Tosun et al., 2014), our results also suggest that for the attribution of CBF reductions to Aβ, tau pathology needs to be taken into account. As a note of caution, however, the current study design does not allow for a causative interpretation of any effects of tau pathology, and thus our findings neither address the directionality nor answer the question which specific pathology is causing CBF changes.

The mechanisms linking local tau pathology to local perfusion are not established yet. A potential candidate mechanism includes tau pathology to cause vascular changes that in turn lead to hypoperfusion. A recent study in transgenic mouse model of neurofibrillary tangles showed structural microvascular abnormalities and disrupted blood flow that was associated with neurodegeneration (Bennett et al., 2018). In brain tissue from both transgenic mice of tau pathology and brain tissue from AD patients, tau pathology was associated with alterations in RNA expression linked to vascular function and hypoxia. In contrast, those changes were not observed in a transgenic mouse model of Aβ (Bennett et al., 2018). These observations in mice and humans suggest that tau pathology may directly impinge upon the microvasculature and thus reduced hypoperfusion. However, lower perfusion may also cause the pathologic tau accumulation as chronic hypoperfusion has been found to be associated with higher phosphorylated tau and Aβ oligomers in rodents (Park et al., 2019). Yet, in nondemented elderly individuals with chronic hypoperfusion due to unilateral artery occlusion showed neither higher amyloid nor tau pathology, suggesting that hypoperfusion may not be eliciting AD pathology (Hansson et al., 2018). It should be noted though that the sample was small, with only 5 individuals receiving tau-PET, and thus the cause of events in humans remains to be established. A third possibility is that tau pathology causes GM atrophy which in turn reduces perfusion. However, other studies using combined structural MRI and ASL changes reported spatially divergent patterns of CBF reduction and GM atrophy in MCI and AD (Tosun et al., 2014; Wirth et al., 2017), supporting the view that CBF alterations do not occur merely as a function of neurodegeneration. In the current study, correction for PVE did not alter the results, thus, while the influence of GM atrophy on CBF changes cannot be excluded, it is unlikely that CBF changes can be reduced to GM atrophy.

Previous study reported increased tau-PET levels in subjects with SVD (Kim et al., 2018). Because SVD is associated with reduced cerebral perfusion (Shi et al., 2016), it is possible that any association between tau and lower perfusion is mediated due to SVD. However, we found no association between SVD markers and CBF in contrast to previous reports of an association between lower perfusion and higher number of microbleeds in nondemented elderlies (Gregg et al., 2015). A potential cause for the discrepancies in the findings is the relatively lower number of microbleeds in the current study compared to that in the previous study. For WMH, findings have been inconsistent, where the latter study reported no association between WMH and CBF (Gregg et al., 2015), but a positive association was reported in nondemented individuals in other studies (Kim et al., 2020). We note that there is currently no direct biomarker of SVD available, rather proxy measure such as WMH and microbleeds provide only crude measures of SVD in vivo. While we found no evidence supporting a role of SVD in the association between tau pathology and CBF, we cation that the current study was not tailored to test these associations. Moreover, since we focused only on grey matter perfusion, we cannot exclude the effect of SVD on perfusion in the white matter. Therefore, the role of SVD in tau associated decreases in perfusion in human remains to be tested.

Some limitations of this study should be considered. First, our study design was cross-sectional and not longitudinal, therefore we could not determine the temporal relationships between tau and CBF changes. Second, ADNI is a multi-site study and as such is susceptible to variability across sites. Therefore, we limited the current study to data acquired on a single scanner and all regression models were controlled for study site effects. Third, pCASL is currently the recommended ASL method by the ISMRM Perfusion Study Group and European Consortium for ASL in Dementia due to its relatively high signal-to-noise ratio (SNR) and clinical applicability (Alsop et al., 2015). However, the hemodynamic status of each individual cannot be precisely estimated using the current method and therefore the quantitative values of CBF may not be accurate. Optimizations of pCASL, such as multi-phase sequences, can collect data in multiple time phases and therefore may offer a more accurate CBF measure (Sugimori et al., 2015). Fourth, the sample size of the AD dementia group in our study was relatively small and most of the subjects were nondemented with

relatively low levels of tau-PET (Johnson et al., 2016; Jack et al., 2017). Enrichment of the sample with subjects with more advanced tau pathology, may have resulted in higher sensitivity to detect associations between CBF and tau-PET not only in the entorhinal cortex but also higher cortical areas. Lastly, we investigated only linear associations between CBF vs amyloid- or tau-PET. Previous studies reported - apart from decreases - also increases in CBF (Wierenga et al., 2012; Beason-Held et al., 2013; Fazlollahi et al., 2020), suggesting that changes in CBF are complex in AD. However, the results of those previous studies were inconsistent with regard to which specific brain regions and clinical phases are linked to increased CBF (Wierenga et al., 2014), and several studies did not report any increases in CBF in MCI (Binnewijzend et al., 2013; Wirth et al., 2017) or AD dementia (Chen et al., 2011; Binnewijzend et al., 2013) at all. In the current study, we observed only inverse associations between CBF and tau-PET or amyloid-PET. The current sample size did not allow to model nonlinear relationships or analyses stratified by clinical subgroup, and thus nonlinear relationships with tau-PET remain to be investigated.

5. Conclusion

In conclusion, decreases in regional CBF can be observed not only in an amyloid-PET manner but also tau-PET dependent, preferentially in regions of high tau-PET uptake. These associations are detectable at an early stage of tau pathology in the absence of clinical dementia as well as in later AD stages and are independent of Aβ pathology, APOE genotype or SVD markers. Thus, CBF measured by pCASL could potentially identify tau- associated CBF alterations in preclinical phase and serve as a noninvasive biomarker for the early detection of AD.

Declaration of competing interest

None.

Author disclosures

Dr. Weiner served on Advisory Boards for Eli Lilly, Cerecin/Accera, Roche, Alzheon, Inc., Merck Sharp & Dohme Corp., Nestle/Nestec, PCORI/PPRN, Dolby Family Ventures, Brain Health Registry and ADNI. He serves on the Editorial Boards for Alzheimer's & Dementia and MRI. He has provided consulting and/or acted as a speaker/lecturer to Cerecin/Accera, Inc., Alzheimer's Drug Discovery Foundation (ADDF), Merck, BioClinica, Eli Lilly, Indiana University, Howard University, Nestle/Nestec, Roche, Genentech, NIH, Lynch Group GLC, Health & Wellness Partners, Bionest Partners, American Academy of Neurology (AAN), and Society for Nuclear Medicine and Molecular Imaging (SNMMI). He holds stock options with Alzheon, Inc.

Acknowledgements

The study was supported by the German Center for Neurodegenerative Diseases (DZNE), Alzheimer Forschung Initiative (AFI, Grant 15035 to ME), LMUexcellent (to ME) and by the Deutsche Forschungsgemeinschaft (DFG, German Research Foundation) grant for major research instrumentation (DFG, INST 409/193-1 FUGG). ADNI data collection and sharing for this project was funded by the ADNI (National Institutes of Health Grant U01 AG024904) and DOD ADNI (Department of Defense award number W81XWH-12-2-0012). ADNI is funded by the National Institute on Aging, the National Institute of Biomedical Imaging, and Bioengineering, and through contributions from the following: AbbVie, Alzheimer's Association; Alzheimer's Drug Discovery Foundation; Araclon Biotech; BioClinica, Inc.; Biogen; Bristol-Myers Squibb Company; CereSpir, Inc.; Cogstate; Eisai Inc.; Elan Pharmaceuticals, Inc.; Eli Lilly and Company; EuroImmun; F. Hoffmann-La Roche Ltd and its affiliated company Genentech, Inc.; Fujirebio; GE Healthcare; IXICO Ltd.; Janssen Alzheimer Immunotherapy Research & Development, LLC.; Johnson & Johnson Pharmaceutical Research & Development LLC.; Lumosity; Lundbeck; Merck & Co., Inc.; Meso Scale Diagnostics, LLC.; NeuroRx Research; Neurotrack Technologies; Novartis Pharmaceuticals Corporation; Pfizer Inc.; Piramal Imaging; Servier; Takeda Pharmaceutical Company; and Transition Therapeutics. The Canadian Institutes of Health Research is providing funds to support ADNI clinical sites in Canada. Private sector contributions are facilitated by the Foundation for the National Institutes of Health (www.fnih.org).

Dr. Weiner receives support for his work from the following funding sources:

NIH, DOD, PCORI, California Dept. of Public Health, U. Michigan, Siemens, Biogen, Hillblom Foundation, Alzheimer's Association. He also receives support from Johnson & Johnson, Kevin and Connie Shanahan, GE, VUmc, Australian Catholic University, The Stroke Foundation, and the Veterans Administration.

Author contributions

AR designed the study, conducted the analyses, interpreted the results and drafted the manuscript, DT analyzed the data and provided critical review of the manuscript, NF and JN provided critical review of the manuscript, LF processed the data, MW provided critical review of the manuscript, ME designed the study, interpreted the results and drafted the manuscript.

Supplementary materials

Supplementary material associated with this article can be found, in the online version, at doi:10.1016/j.neurobiolaging.2021.02.003.

References

Alsop, D.C., Detre, J.A., Golay, X., Günther, M., Hendrikse, J., Hernandez-Garcia, L., Lu, H., MacIntosh, B.J., Parkes, L.M., Smits, M., van Osch, M.J.P., Wang, D.J.J., Wong, E.C., Zaharchuk, G., 2015. Recommended implementation of arterial spin-labeled perfusion MRI for clinical applications: A consensus of the ISMRM perfusion study group and the European consortium for ASL in dementia. Magn Reson Med 73 (1), 102–116.

Asllani, I., Borogovac, A., Brown, T.R., 2008. Regression algorithm correcting for partial volume effects in arterial spin labeling MRI. Magn Reson Med 60 (6), 1362–1371.

Baker, S.L., Maass, A., Jagust, W.J., 2017. Considerations and code for partial volume correcting [(18)F]-AV-1451 tau PET data. Data in Brief 15, 648–657.

Bangen, K.J., Clark, A.L., Edmonds, E.C., Evangelista, N.D., Werhane, M.L., Thomas, K.R., Locano, L.E., Tran, M., Zlatar, Z.Z., Nation, D.A., Bondi, M.W., Delano-Wood, L., 2017. Cerebral blood flow and amyloid-beta interact to affect memory performance in cognitively normal older adults. Front Aging Neurosci 9, 181.

Beason-Held, L.L., Goh, J.O., An, Y., Kraut, M.A., O'Brien, R.J., Ferrucci, L., Resnick, S.M., 2013. Changes in brain function occur years before the onset of cognitive impairment. J Neurosci 33 (46), 18008–18014.

Bennett, R.E., Robbins, A.B., Hu, M., Cao, X., Betensky, R.A., Clark, T., Das, S., Hyman, B.T., 2018. Tau induces blood vessel abnormalities and angiogenesis-related gene expression in P301L transgenic mice and human Alzheimer's disease. Proc Natl Acad Sci U S A 115 (6), E1289–E1E98.

Binnewijzend, M.A., Benedictus, M.R., Kuijer, J.P., van der Flier, W.M., Teunissen, C.E., Prins, N.D., Wattjes, M.P., van Berckel, B.N., Scheltens, P., Barkhof, F., 2016. Cerebral perfusion in the predementia stages of Alzheimer's disease. Eur Radiol 26 (2), 506–514.

Binnewijzend, M.A., Kuijer, J.P., Benedictus, M.R., van der Flier, W.M., Wink, A.M., Wattjes, M.P., van Berckel, B.N., Scheltens, P., Barkhof, F., 2013. Cerebral blood flow measured with 3D pseudocontinuous arterial spin-labeling MR imaging in Alzheimer disease and mild cognitive impairment: a marker for disease severity. Radiology 267 (1), 221–230.

Bollen, K.A., Jackman, R.W., 1985. Regression diagnostics: an expository treatment of outliers and influential cases. Sociolog Methods Res 13 (4), 510–542.

Bradley, K.M., O'Sullivan, V.T., Soper, N.D.W., Nagy, Z., King, E.M.F., Smith, A.D., Shepstone, B.J., 2002. Cerebral perfusion SPET correlated with Braak pathological stage in Alzheimer's disease. Brain 125 (8), 1772–1781.
Caballero, M.ÁA., Song, Z., Rubinski, A., Duering, M., Dichgans, M., Park, D.C., Ewers, M., 2020. Age-dependent amyloid deposition is associated with white matter alterations in cognitively normal adults during the adult life span. Alzheimer's Dementia n/a(n/a.
Chao, L.L., Buckley, S.T., Kornak, J., Schuff, N., Madison, C., Yaffe, K., Miller, B.L., Kramer, J.H., Weiner, M.W., 2010. ASL perfusion MRI predicts cognitive decline and conversion from MCI to dementia. Alzheimer Dis Assoc Disord 24 (1), 19–27.
Chen, Y., Wolk, D.A., Reddin, J.S., Korczykowski, M., Martinez, P.M., Musiek, E.S., Newberg, A.B., Julin, P., Arnold, S.E., Greenberg, J.H., Detre, J.A., 2011. Voxel-level comparison of arterial spin-labeled perfusion MRI and FDG-PET in Alzheimer disease. Neurology 77 (22), 1977–1985.
Cook, R.D., Weisberg, S., 1982. Residuals and influence in regression. Chapman and Hall, New York.
Desikan, R.S., Ségonne, F., Fischl, B., Quinn, B.T., Dickerson, B.C., Blacker, D., Buckner, R.L., Dale, A.M., Maguire, R.P., Hyman, B.T., Albert, M.S., Killiany, R.J., 2006. An automated labeling system for subdividing the human cerebral cortex on MRI scans into gyral based regions of interest. NeuroImage 31 (3), 968–980.
Fazlollahi, A., Calamante, F., Liang, X., Bourgeat, P., Raniga, P., Dore, V., Fripp, J., Ames, D., Maters, C.L., Rowe, C.C., Connelly, A., Villemagne, V.L., Salvado, O.Australian Imaging Biomarkers and Lifestyle (AIBL) Research Group, 2020. Increased cerebral blood flow with increased amyloid burden in the preclinical phase of alzheimer's disease. J Magn Reson Imaging 51 (2), 505–513.
Gregg, N.M., Kim, A.E., Gurol, M.E., Lopez, O.L., Aizenstein, H.J., Price, J.C., Mathis, C.A., James, J.A., Snitz, B.E., Cohen, A.D., Kamboh, M.I., Minhas, D., Weissfeld, L.A., Tamburo, E.L., Klunk, W.E., 2015. Incidental cerebral microbleeds and cerebral blood flow in elderly individuals. JAMA Neurol 72 (9), 1021–1028.
Habert, M.-O., de Souza, L.C., Lamari, F., Daragon, N., Desarnaud, S., Jardel, C., Dubois, B., Sarazin, M., 2010. Brain perfusion SPECT correlates with CSF biomarkers in Alzheimer's disease. Eur J Nuclear Med Mol Imaging 37 (3), 589–593.
Hansson, O., Palmqvist, S., Ljung, H., Cronberg, T., van Westen, D., Smith, R., 2018. Cerebral hypoperfusion is not associated with an increase in amyloid β pathology in middle-aged or elderly people. Alzheimer's Dementia 14 (1), 54–61.
Hays, C.C., Zlatar, Z.Z., Meloy, M.J., Osuna, J., Liu, T.T., Galasko, D.R., Wierenga, C.E., 2020. Anterior cingulate structure and perfusion is associated with cerebrospinal fluid tau among cognitively normal older adult APOEvarepsilon4 carriers. J Alzheimer's Dis 73 (1), 87–101.
Jr. Jack Jr., C.R., Wiste, H.J., Schwarz, C.G., Lowe, V.J., Senjem, M.L., Vemuri, P., Weigand, S.D., Therneau, T.M., Knopman, D.S., Gunter, J.L., Jones, D.T., Graff-Radford, J, Kantarci, K., Roberts, R.O., Mielke, M.M., Machulda, M.M., Petersen, R.C., 2018. Longitudinal tau PET in ageing and Alzheimer's disease. Brain 141 (5), 1517–1528.
Jr. Jack Jr., C.R., Wiste, H.J., Weigand, S.D., Therneau, T.M., Lowe, V.J., Knopman, D.S., Gunter, J.L., Senjem, M.L., Jones, D.T., Kantarci, K., Machulda, M.M., Mielke, M.M., Roberts, R.O., Vemuri, P, Reyes, D.A., Petersen, R.C., 2017. Defining imaging biomarker cut points for brain aging and Alzheimer's disease. Alzheimer's Dementia 13 (3), 205–216.
Jagust, W.J., Landau, S.M., Koeppe, R.A., Reiman, E.M., Chen, K., Mathis, C.A., Price, J.C., Foster, N.L., Wang, A.Y., 2015. The ADNI PET Core: 2015. Alzheimer's & dementia: the journal of the. Alzheimer's Assoc 11 (7), 757–771.
Johnson, K.A., Schultz, A., Betensky, R.A., Becker, J.A., Sepulcre, J., Rentz, D., Mormino, E., Chhatwal, J., Amariglio, R., Rapp, K., Marshall, G., Albers, M., Mauro, S., Pepin, L., Alverio, J., Judge, K., Philiossaint, M., Shoup, T., Yokell, D., Dickerson, B., Gomez-Isla, T., Hyman, B., Vasdev, N., Sperling, R., 2016. Tau PET imaging in aging and early Alzheimer's disease. Ann Neurol 79 (1), 110–119.
Kim, C.M., Alvarado, R.L., Stephens, K., Wey, H.Y., Wang, D.J.J., Leritz, E.C., Salat, D.H., 2020. Associations between cerebral blood flow and structural and functional brain imaging measures in individuals with neuropsychologically defined mild cognitive impairment. Neurobiol Aging 86, 64–74.
Kim, H.J., Park, S., Cho, H., Jang, Y.K., San Lee, J., Jang, H., Kim, Y., Kim, K.W., Ryu, Y.H., Choi, J.Y., Moon, S.H., Weiner, M.W., Jagust, W.J., Rabinovici, G.D., DeCarli, C., Lyoo, C.H., Na, D.L., Seo, S.W., 2018. Assessment of extent and role of tau in subcortical vascular cognitive impairment using 18F-AV1451 positron emission tomography imaging. JAMA Neurol 75 (8), 999–1007.
Landau, S.M., Mintun, M.A., Joshi, A.D., Koeppe, R.A., Petersen, R.C., Aisen, P.S., Weiner, M.W., Jagust, W.J., 2012. Amyloid deposition, hypometabolism, and longitudinal cognitive decline. Ann Neurol 72 (4), 578–586.
Love, S., Miners, J.S., 2016. Cerebrovascular disease in ageing and Alzheimer's disease. Acta Neuropathol 131 (5), 645–658.
Maass, A., Landau, S., Baker, S.L., Horng, A., Lockhart, S.N., La Joie, R., Rabinovici, G.D., Jagust, W.J., 2017. Comparison of multiple tau-PET measures as biomarkers in aging and Alzheimer's disease. Neuroimage 157, 448–463.
Marquie, M., Normandin, M.D., Vanderburg, C.R., Costantino, I.M., Bien, E.A., Rycyna, L.G., Klunk, W.E., Mathis, C.A., Ikonomovic, M.D., Debnath, M.L., Vadev, N., Dickerson, B.C., Gomperts, S.N., Growdon, J.H., Johnson, K.A., Frosch, M.P., Hyman, B.T., Gomez-Isla, T., 2015. Validating novel tau positron emission tomography tracer [F-18]-AV-1451 (T807) on postmortem brain tissue. Ann Neurol 78 (5), 787–800.
Jr. Mattsson, N., Tosun, D., Insel, P.S., Simonson, A., Jack, C.R., Beckett, L.A., Donohue, M., Jagust, W., Schuff, N., Weiner, M.W.Alzheimer's Disease Neuroimaging Initiative, 2014. Association of brain amyloid-β with cerebral perfusion and structure in Alzheimer's disease and mild cognitive impairment. Brain 137, 1550–1561 (Pt 5).
McDade, E., Kim, A., James, J., Sheu, L.K., Kuan, DC-H., Minhas, D., Gianaros, P.J., Ikonomovic, S., Lopez, O., Snitz, B., Price, J., Becker, J., Mathis, C., Klunk, W., 2014. Cerebral perfusion alterations and cerebral amyloid in autosomal dominant Alzheimer disease. Neurology 83 (8), 710.
Michels, L., Warnock, G., Buck, A., Macauda, G., Leh, S.E., Kaelin, A.M., Riese, F., Meyer, R., O'Gorman, R., Hock, C., Kollias, S., Gietl, A.F., 2016. Arterial spin labeling imaging reveals widespread and Abeta-independent reductions in cerebral blood flow in elderly apolipoprotein epsilon-4 carriers. J Cerebral Blood Flow Metab 36 (3), 581–595.
Mutsaerts, H.J.M.M., Petr, J., Groot, P., Vandemaele, P., Ingala, S., Robertson, A.D., Václavů, L., Groote, I., Kuijf, H., Zelaya, F., O'Daly, O., Hilal, S., Wink, A.M., Kant, I., Caan, M.W.A., Morgan, C., de Bresser, J., Lysvik, E., Schrantee, A., Bjørnebekk, A., Clement, P., Shirzadi, Z., Kuijer, J.P.A., Wottschel, V., Anazodo, U.C., Pajkrt, D., Richard, E., Bokkers, R.P.H., Reneman, L., Masellis, M., Günther, M., MacIntosh, B.J., Achten, E., Chappell, M.A., van Osch, M.J.P., Golay, X., Thomas, D.L., De Vita, E., Bjørnerud, A., Nederveen, A., Hendrikse, J., Asllani, I., Barkhof, F., 2020. ExploreASL: An image processing pipeline for multi-center ASL perfusion MRI studies. NeuroImage 219, 117031.
Palmqvist, S., Schöll, M., Strandberg, O., Mattsson, N., Stomrud, E., Zetterberg, H., Blennow, K., Landau, S., Jagust, W., Hansson, O., 2017. Earliest accumulation of β-amyloid occurs within the default-mode network and concurrently affects brain connectivity. Nat Commun 8 (1), 1214.
Park, J.H., Hong, J.H., Lee, S.W., Ji, H.D., Jung, J.A., Yoon, K.W., Lee, J.I., Won, K.S., Song, B.I., Kim, H.W., 2019. The effect of chronic cerebral hypoperfusion on the pathology of Alzheimer's disease: A positron emission tomography study in rats. Sci Rep 9 (1), 14102.
Petersen, R.C., Aisen, P.S., Beckett, L.A., Donohue, M.C., Gamst, A.C., Harvey, D.J., Jack, C.R., Jagust, W.J., Shaw, L.M., Toga, A.W., Trojanowski, J.Q., Weiner, M.W., 2010. Alzheimer's Disease Neuroimaging Initiative (ADNI): clinical characterization. Neurology 74 (3), 201–209.
Petr, J., Mutsaerts, H.J.M.M., De Vita, E., Steketee, R.M.E., Smits, M., Nederveen, A.J., Hofheinz, F., van den Hoff, J., Asllani, I, 2018. Effects of systematic partial volume errors on the estimation of gray matter cerebral blood flow with arterial spin labeling MRI. Magnetic Resonance Materials in Physics. Biol Med 31 (6), 725–734.
Rodell, A.B., O'Keefe, G., Rowe, C.C., Villemagne, V.L., Gjedde, A., 2016. Cerebral blood flow and a beta-amyloid estimates by WARM analysis of [(11)C]PiB uptake distinguish among and between neurodegenerative disorders and aging. Front Aging Neurosci 8, 321.
Shi, Y., Thrippleton, M.J., Makin, S.D., Marshall, I., Geerlings, M.I., de Craen, A.J.M., van Buchem, M.A., Wardlaw, J.M., 2016. Cerebral blood flow in small vessel disease: A systematic review and meta-analysis. J Cerebral Blood Flow Metab 36 (10), 1653–1667.
Stomrud, E., Forsberg, A., Hägerström, D., Ryding, E., Blennow, K., Zetterberg, H., Minthon, L., Hansson, O., Londos, E., 2012. CSF biomarkers correlate with cerebral blood flow on SPECT in healthy elderly. Dement Geriatric Cognit Disord 33 (2–3), 156–163.
Sugimori, H., Fujima, N., Suzuki, Y., Hamaguchi, H., Sakata, M., Kudo, K., 2015. Evaluation of cerebral blood flow using multi-phase pseudo continuous arterial spin labeling at 3-tesla. Magn Reson Imaging 33 (10), 1338–1344.
Thomas, T., Miners, S., Love, S., 2015. Post-mortem assessment of hypoperfusion of cerebral cortex in Alzheimer's disease and vascular dementia. Brain 138, 1059–1069 (Pt 4).
Tosun, D., Joshi, S., Weiner, M.W.Alzheimer's Disease Neuroimaging Initiative, 2014. Multimodal MRI-based imputation of the Abeta+ in early mild cognitive impairment. Ann Clin Transl Neurol 1 (3), 160–170.
Tosun, D., Schuff, N., Rabinovici, G.D., Ayakta, N., Miller, B.L., Jagust, W., Kramer, J., Weiner, M.M., Rosen, H.J., 2016. Diagnostic utility of ASL-MRI and FDG-PET in the behavioral variant of FTD and AD. Ann Clin Transl Neurol 3 (10), 740–751.
Wierenga, C.E., Dev, S.I., Shin, D.D., Clark, L.R., Bangen, K.J., Jak, A.J., Rissman, R.A., Liu, T.T., Salmon, D.P., Bondi, M.W., 2012. Effect of mild cognitive impairment and APOE genotype on resting cerebral blood flow and its association with cognition. J Cerebral Blood Flow Metab 32 (8), 1589–1599.
Wierenga, C.E., Hays, C.C., Zlatar, Z.Z., 2014. Cerebral blood flow measured by arterial spin labeling MRI as a preclinical marker of Alzheimer's disease. J Alzheimer's Dis 42 (Suppl 4), S411–S419.
Wirth, M., Pichet Binette, A., Brunecker, P., Kobe, T., Witte, A.V., Floel, A., 2017. Divergent regional patterns of cerebral hypoperfusion and gray matter atrophy in mild cognitive impairment patients. J Cerebral Blood Flow Metab 37 (3), 814–824.
Wolf, R.L., Detre, J.A., 2007. Clinical neuroimaging using arterial spin-labeled perfusion magnetic resonance imaging. Neurotherapeutics 4 (3), 346–359.
Wolters, F.J., Zonneveld, H.I., Hofman, A., van der Lugt, A., Koudstaal, P.J., Vernooij, M.W., Ikram, M.A.Heart-Brain Connection Collaborative Research Group, 2017. Cerebral perfusion and the risk of dementia: a population-based study. Circulation 136 (8), 719–728.
Xekardaki, A., Rodriguez, C., Montandon, M.L., Toma, S., Tombeur, E., Herrmann, F.R., Zekry, D., Lovbald, K.O., Barkhof, F., Giannakopoulos, P., Haller, S., 2015. Arterial spin labeling may contribute to the prediction of cognitive deterioration in healthy elderly individuals. Radiology 274 (2), 490–499.
Yew, B., Nation, D.A., 2017. Alzheimer's Disease Neuroimaging I. Cerebrovascular resistance: effects on cognitive decline, cortical atrophy, and progression to dementia. Brain 140 (7), 1987–2001.

Supplementary

Supplementary Table 1: Sub-analyses of linear mixed models testing the effects of tau-PET on CBF.

Model terms	Braak I		Braak III/IV		Braak V/VI	
	b/SE	*p*	*b*/SE	*p*	*b*/SE	*p*
Aβ+ subjects (n=58): Main effect - Regional Tau-PET						
Tau	-0.485/0.139	0.001	0.106/0.150	0.483	-0.107/0.132	0.422
Aβ- subjects (n=87): Main effect - Regional Tau-PET						
Tau	-0.313/0.095	0.002	-0.238/0.109	0.032	0.021/0.118	0.857
Non-demented subgroup (n=138): Main effect - Regional Tau-PET						
Tau	-0.236/0.086	0.007	-0.095/0.089	0.287	-0.111/0.088	0.208
Amyloid subset (n=145): Main effect - Regional Tau-PET + Regional amyloid-PET centiloid						
Tau	-0.363/0.095	<0.001	-0.040/0.102	0.694	-0.067/0.089	0.451
Aβ	0.077/0.084	0.359	-0.168/0.098	0.089	-0.229/0.089	0.012
Amyloid subset (n=145): Interaction- Regional Tau-PET x Regional amyloid-PET centiloid						
Tau	-0.346/0.096	<0.001	0.017/0.172	0.920	0.273/0.191	0.155
Aβ	-0.297/0.282	0.294	0.010/0.438	0.981	0.609/0.425	0.154
Tau x Aβ	0.379/0.273	0.166	-0.221/0.529	0.676	-1.059/0.526	0.461
APOE subset (n=140): Main effect - Regional Tau-PET + APOE status						
Tau	-0.412/0.095	<0.001	-0.109/0.097	0.261	-0.119/0.089	0.182
APOE	0.039/0.082	0.639	-0.062/0.089	0.487	-0.102/0.083	0.222
APOE e4- subjects (n=83): Main effect - Regional Tau-PET						
Tau	-0.397/0.111	<0.001	-0.146/0.116	0.210	-0.011/0.118	0.923
APOE e4+ subjects (n=57): Main effect - Regional Tau-PET						
Tau	-0.372/0.162	0.026	-0.029/0.153	0.849	-0.119/0.138	0.392
APOE subset (n=140): Interaction: Regional Tau-PET x APOE status						
Tau	-0.469/0.127	<0.001	-0.200/0.194	0.304	0.004/0.265	0.987
APOE	-0.130/0.261	0.619	-0.284/0.420	0.501	0.172/0.569	0.763
Tau x APOE	0.203/0.298	0.498	0.269/0.498	0.590	-0.333/0.681	0.625

Models are controlled for age, gender, education, diagnosis (fixed effects) and study site (random effect)

Supplementary Table 2: Sub-analyses of linear mixed models testing the effects of amyloid-PET on CBF.

Model terms	Inferior temporal		Parahippocampus		Inferior parietal		Posterior cingulate		Precuneus		Medial orbitofrontal	
	b/SE	*p*	*b*/SE	*p*	*b*/SE	*p*	*b*/SE	*p*	*b*/SE	*p*	*b*/SE	*p*
Amyloid subset (n=145): Main effect - Global amyloid-PET + regional Tau-PET												
Aβ	-0.291/0.095	0.003	-0.108/0.110	0.330	-0.117/0.080	0.149	0.010/0.092	0.912	-0.184/0.091	0.044	-0.025/0.085	0.773
Tau	-0.155/0.098	0.116	0.026/0.112	0.821	-0.336/0.083	<0.001	0.093/0.091	0.310	-0.087/0.089	0.324	-0.062/0.083	0.462
Amyloid subset (n=145): Main effect - Regional amyloid-PET centiloid												
Aβ	-0.288/0.085	<0.001	-0.092/0.087	0.292	-0.243/0.076	0.002	0.042/0.084	0.617	-0.207/0.084	0.015	-0.036/0.083	0.660

Models are controlled for age, gender, education, diagnosis (fixed effects) and study site (random effect)

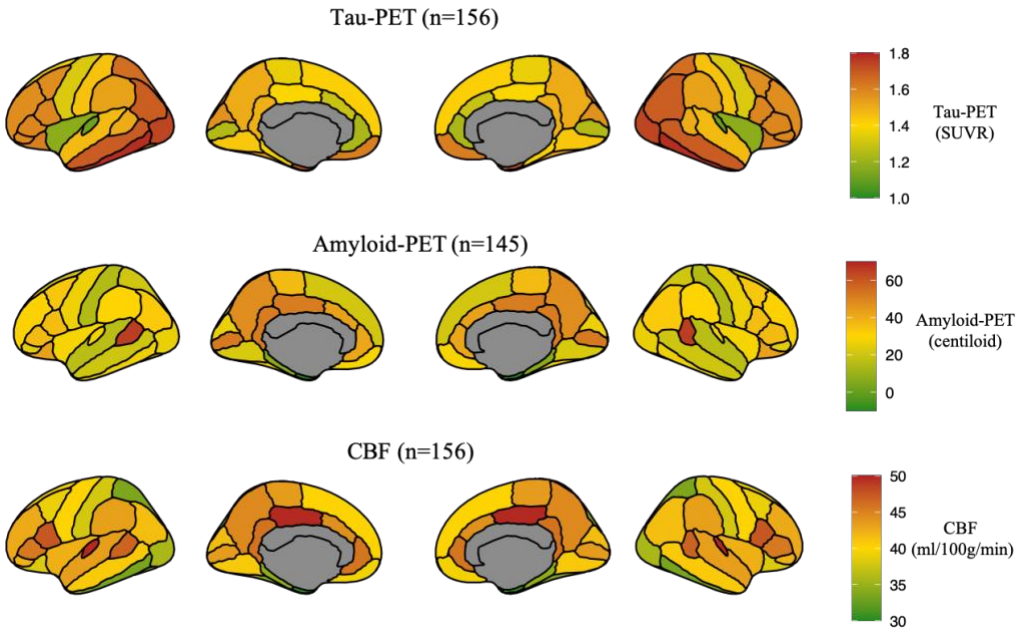

Supplementary Figure 1: Spatial mapping of amyloid-PET centiloid, tau-PET SUVR, and CBF distribution

Manuscript 3

Neitzel, J., Franzmeier, N., **Rubinski, A.,** Ewers, M., & Alzheimer's Disease Neuroimaging Initiative (ADNI). (2019). Left frontal connectivity attenuates the adverse effect of entorhinal tau pathology on memory. *Neurology, 93*(4), e347-e357.

DOI: 10.1212/WNL.0000000000007822

Contributions: AR managed and processed the data, revised the manuscript, JN designed and conceptualized study, analyzed and interpreted the data, drafted the manuscript, NF interpreted the data, revised the manuscript, ME designed and conceptualized study, interpreted the data, and drafted the manuscript.

Acknowledgements

I would like first to thank my supervisor, Prof. Dr. Michael Ewers, for his guidance and support throughout my PhD. I would also like to thank the rest of my thesis committee, Prof. Dr. med. Marco Düring and PD Dr. med. Igor Yakushev, for their helpful feedback to improve this work.

Further, I would like to thank all co-authors and colleagues for their valuable contribution and support throughout the development of this dissertation.

Finally, I would like to thank my family, friends, and partner who supported and encouraged me throughout this long journey.

List of publications

Rubinski, A., Tosun, D., Franzmeier, N., Neitzel, J., Frontzkowski, L., Weiner, M., & Ewers, M. (2021). Lower cerebral perfusion is associated with tau-PET in the entorhinal cortex across the Alzheimer's continuum. *Neurobiology of Aging, 102*, 111-118.

Rubinski, A., Franzmeier, N., Neitzel, J., & Ewers, M. (2020). FDG-PET hypermetabolism is associated with higher tau-PET in mild cognitive impairment at low amyloid-PET levels. *Alzheimer's research & therapy, 12*(1), 1-12.

Franzmeier, N., Dewenter, A., Frontzkowski, L., Dichgans, M., **Rubinski, A.**, …, Ewers, M. (2020). Patient-centered connectivity-based prediction of tau pathology spread in Alzheimer's disease. *Science Advances, 6*(48), eabd1327.

Caballero, M.A.A., Song, Z., **Rubinski, A.**, Duering, M., Dichgans, M., Park, D.C., Ewers, M. (2020). Age-dependent amyloid deposition is associated with white matter alterations in cognitively normal adults during the adult life span. *Alzheimer's and Dementia, 16*(4), 651-661.

Franzmeier, N., Neitzel, J., **Rubinski, A.,** Smith, R., Strandberg, O., Ossenkoppele, R., Hansson, O., Ewers, M. (2020). Functional brain architecture is associated with the rate of tau accumulation in Alzheimer's disease. *Nature Communications, 11(1), 1-17.*

Franzmeier, N., **Rubinski, A.**, Neitzel, J., Ewers, M. (2019). The BIN1 rs744373 SNP is associated with increased tau-PET levels and impaired memory. *Nature Communications*, *10*(1), 1-12.

Neitzel, J., Franzmeier, N., **Rubinski, A.,** Ewers, M., & Alzheimer's Disease Neuroimaging Initiative (ADNI). (2019). Left frontal connectivity attenuates the adverse effect of entorhinal tau pathology on memory. *Neurology, 93*(4), e347-e357.

Franzmeier, N., **Rubinski, A.,** ..., Ewers, M. (2019). Functional connectivity associated with tau levels in aging, Alzheimer's and small-vessel disease. *Brain*, *142*(4), 1093-1107.

Affidavit

I hereby declare that the submitted thesis entitled:

Effects of Amyloid and Tau pathology on brain function and cognition in Alzheimer's disease

is my own work. I have only used the sources indicated and have not made unauthorised use of services of a third party. Where the work of others has been quoted or reproduced, the source is always given.

I further declare that the submitted thesis or parts thereof have not been presented as part of an examination degree to any other university.

Munich, 25.10.2021	Anna Rubinski
Place, date	Signature

Confirmation of congruency

I hereby declare that the electronic version of the submitted thesis entitled:

Effects of Amyloid and Tau pathology on brain function and cognition in Alzheimer's disease

is congruent with the printed version both in content and format.

Munich, 25.10.2021	Anna Rubinski
Place, date	Signature